AD-A032 177 AEROSPACE CORP EL SEGUNDO CALIF ENGINEERING SCIENCE --ETC F/G 9/5
ALUMINA SUBSTRATE ASSEMBLY STUDY.(U)
OCT 76 J H RICHARDSON F04701-76-C-0077
UNCLASSIFIED TR-0077(2724-01)-1 SAMSO-TR-76-214 NL

1 OF 1
AD A032177

END

DATE FILMED
1-77

REPORT SAMSO-TR-76-214

12

Alumina Substrate Assembly Study

Engineering Science Operations
The Aerospace Corporation
El Segundo, Calif. 90245

1 October 1976

Final Report

Prepared for

SPACE AND MISSILE SYSTEMS ORGANIZATION
AIR FORCE SYSTEMS COMMAND
Los Angeles Air Force Station
P.O. Box 92960, Worldway Postal Center
Los Angeles, Calif. 90009

THE AEROSPACE CORPORATION

This final report was submitted by The Aerospace Corporation, El Segundo CA 90245, under Contract F04701-76-C-0077 with the Space and Missile Systems Organization, Deputy for Space Communications Systems, P. O. Box 92960, Worldway Postal Center, Los Angeles CA 90009. It was reviewed and approved for The Aerospace Corporation by D. J. Griep, Engineering Science Operations and H. F. Meyer, Systems Engineering Operations. 1st Lt. Martin P. Hopper, SAMSO/SKF, was the project engineer.

This report has been reviewed by the Information Office (OIS) and is releasable to the National Technical Information Service (NTIS). At NTIS, it will be available to the general public, including foreign nations.

This technical report has been reviewed and is approved for publication. Publication of this report does not constitute Air Force approval of the report's findings or conclusions. It is published only for the exchange and stimulation of ideas.

Martin P. Hopper, Jr.

Martin P. Hopper, Jr., 1st Lt. USAF
Project Engineer
FLTSATCOM SPO
Deputy for Space Communications Systems

Jake A. Saltamachia

Jake A. Saltamachia, Lt. Col. USAF
Chief, Manufacturing & Production Engineering
FLTSATCOM SPO
Deputy for Space Communications Systems

FOR THE COMMANDER

Forrest S. McCartney

FORREST S. McCARTNEY, Colonel, USAF
FLTSATCOM System Program Director
Deputy for Space Communications Systems

UNCLASSIFIED

SECURITY CLASSIFICATION OF THIS PAGE (When Data Entered)

REPORT DOCUMENTATION PAGE	READ INSTRUCTIONS BEFORE COMPLETING FORM
1. REPORT NUMBER (19) SAMSO TR-76-214	2. GOVT ACCESSION NO. (9) Final
4. TITLE (and Subtitle) (6) ALUMINA SUBSTRATE ASSEMBLY STUDY,	5. TYPE OF REPORT & PERIOD COVERED Interim Rept.
	6. PERFORMING ORG. REPORT NUMBER (14) TR-0077(2724-01)-1
7. AUTHOR(s) (10) James H. Richardson	8. CONTRACT OR GRANT NUMBER(s) (15) F04701-76-C-0077
9. PERFORMING ORGANIZATION NAME AND ADDRESS The Aerospace Corporation El Segundo, Calif. 90245	10. PROGRAM ELEMENT, PROJECT, TASK AREA & WORK UNIT NUMBERS
11. CONTROLLING OFFICE NAME AND ADDRESS (11) Space and Missile Systems Organization/SK P.O. Box 92960, Worldway Postal Center Los Angeles, Calif. 90009	12. REPORT DATE 1 Oct 1976
	13. NUMBER OF PAGES 84
14. MONITORING AGENCY NAME & ADDRESS (if different from Controlling Office) (12) 84p.	15. SECURITY CLASS. (of this report) Unclassified
	15a. DECLASSIFICATION/DOWNGRADING SCHEDULE

16. DISTRIBUTION STATEMENT (of this Report)

Approved for public release; distribution unlimited.

17. DISTRIBUTION STATEMENT (of the abstract entered in Block 20, if different from Report)

18. SUPPLEMENTARY NOTES

19. KEY WORDS (Continue on reverse side if necessary and identify by block number)

Alumina substrate assembly
ASA
Failure analysis
Mechanical shock testing
Thermal cycle testing
Vibration testing

20. ABSTRACT (Continue on reverse side if necessary and identify by block number)

The potential exists for intermittent electrical failures as the result of the various mission environments experienced by the Alumina Substrate Assemblies (ASAs) used in FLTSATCOM. To explore this possibility, a test program was devised in which samples of the ASA technology were subjected to a series of monitored vibration, mechanical shock, and thermal cycle environments that approximated those of the mission. CONT.

(Abstract continued)

DD FORM 1473 (FACSIMILE)

A044068

UNCLASSIFIED

SECURITY CLASSIFICATION OF THIS PAGE (When Data Entered)

19. KEY WORDS (Continued)

20. ABSTRACT (Continued)

The tests indicated that no failures could be directly attributed to the alumina substrate. Those few failures that did occur were more adequately explained in terms of other failure mechanisms. Therefore, it would appear that the ASA is a viable medium for FLTSATCOM modules when subjected to environments within the range of this study.

PREFACE

The author thanks J. R. Howell, J. J. Egan, and D. L. Fresh of The Aerospace Corporation and P. F. Godwin, Jr. and J. P. Woodward, Jr. of TRW for their helpful comments and discussions. The author is particularly grateful to A. F. Young who constructed the special electronics, monitored the mechanical tests, performed all thermal and electrical tests, and reduced the voluminous data and to J. M. Gardner who prepared cross sections of the piece parts and examined them in the scanning electron microscope.

CONTENTS

FIGURES

FIGURES (Continued)

TABLES

I. INTRODUCTION

TRW is using Alumina Substrate Assembly (ASA) manufacturing techniques in the communications systems of the FLTSATCOM satellite. In support of this approach, TRW Systems had conducted a series of thermal cycle/life tests on representative samples of the ASA technology. However, the test samples were not electrically monitored during these life tests and the question was raised by the FLTSATCOM Program Office as to the possibility of undetected intermittent failures having occurred during the test. The most probable failure mechanism of that type would be an intermittent open in a barium titanate chip capacitor during thermal cycling due to differences in thermal coefficient of expansion between the capacitor and the alumina substrate to which it is soldered. This was established in the previously mentioned nonmonitored tests performed by TRW and is consistent with expected results.

A. OBJECTIVES

In order to explore the possibility of intermittents occurring during thermal cycling, Aerospace was requested to devise and perform a test program aimed specifically at that failure mechanism. In response to this request, a test program was devised in which samples of the ASA technology were subjected to a series of monitored vibration, shock, and thermal cycle environments as described in this report. The approach taken was to subject the test samples to a series of environments that would approximate those seen by the FLTSATCOM satellite during its planned mission in addition to a series of more severe thermal cycles (in terms of both number and stress level) in an attempt to establish the margin between the program requirement and the technology capability.

This was then followed by a series of semidestructive evaluations composed of qualification level vibration shock and thermal cycle testing and

metallographic sectioning evaluations. The mission simulation part of the test program was comprised of some 200 thermal cycles while the following life test portion was composed of 800 thermal cycles. A comparison of the anticipated environmental conditions for the FLTSATCOM vehicle with the conditions experienced during this testing is given in Table 1.

A special test module was designed that was comprised primarily of chip capacitors and included some inductors and resistors. These components were arranged in series networks so as to facilitate electrical monitoring during test. Each module was comprised of two different substrates so that the interconnect technique between the substrates could also be evaluated. A total of three such modules were fabricated for and subjected to this test program. They were manufactured by TRW in such a way as to be representative of the quality and technology to be employed in the FLTSATCOM satellite.

The design of the test program and the test modules was carefully coordinated with the FLTSATCOM Program Office and TRW. TRW, who manufactured the modules, was invited to monitor tests as desired and participate in any failure analysis/rework activities resulting from test failures. All test program anomalies were brought to the attention of the program office and TRW.

B. SUMMARY OF RESULTS

Three ASA modules were subjected to a series of vibration, shock, and thermal cycle environments. Results of these studies indicated that no failures could be directly attributed to the alumina substrate. The failures observed were almost exclusively parts related. Thus, the alumina substrate assembly would seem to be a viable medium for fabrication of electronic modules.

Table 1. Comparison of Test Conditions with Anticipated FLTSATCOM Launch and Orbital Conditions

Environment	Aerospace Tests	FLTSATCOM Specification Qualification Level	Anticipated Launch and Transfer Orbital Conditions	Anticipated Orbital Conditions
Thermal Cycle	200 Cycles (-46°C to +60°C) 800 Cycles (-50°C to +100°C) 5 Cycles (-65°C to +125°C) 5 Cycles (-80°C to +150°C)	4 Cycles -46°C to +60°C	-13°C to +26°C	-5°C to +50°C
Random Vibration	1.0 g^2/hr 6 min/axis -35°C, 20°C, 60°C	0.3 g^2/Hz 3 min/axis 3 axes	0.15 g^2/Hz	Nil
Shock	2500 g peak, 1 shock/axis -35°C, 20°C, 60°C	2500 g peak	<orbit	1750 g peak

II. EXPERIMENTAL

A. ASA MODULE FABRICATION

The components of the ASA modules used in this study are shown in Figure 1. The substrates used by TRW for fabrication of the ASAs are Al Si Mag 777 made by American Lava. This 99.5% Al_2O_3 has a 10 μin. centerline average (CLA) finish and approximately 50 μin. surface roughness. The dimensions of each substrate are 1.7 x 2.0 x 0.5 in. The surfaces of the substrate are coated with sputtered Cr-SiO_x cermet (300-500 Å) and then with gold (3000-5000 Å). One side of the substrate serves as a ground plane and the other side is pattern plated with 400 μin. of copper and 100 μin. of gold for the required circuitry. The pattern is then coated with solder by dipping, which also removes the unwanted gold. The substrate corners are trimmed with a diamond saw, and then the substrate is soldered to a Kovar frame on the ground plane side. This frame is provided with a hole at each corner for mounting to bosses in the microwave assembly housing. The components were soldered in place with 63-37 lead tin solder. Figure 2 is a detailed manufacturing flow diagram for the ASAs. The substrates are connected to each other and the coaxial feedthrough connector termination by nickel ribbon "butterflies" that are joined by 63-37 lead tin solder. A cross section of a substrate with a butterfly is shown in Figure 3.

The documents that were used to govern the fabrication of the ASA modules at TRW are as follows:

Military

MIL-C-14550	Copper Plating (Electrodeposited)
MIL-I-23011	Iron-Nickel Alloys for Sealing to Glasses and Ceramics
MIL-G-45204	Gold Plating, Electrodeposited

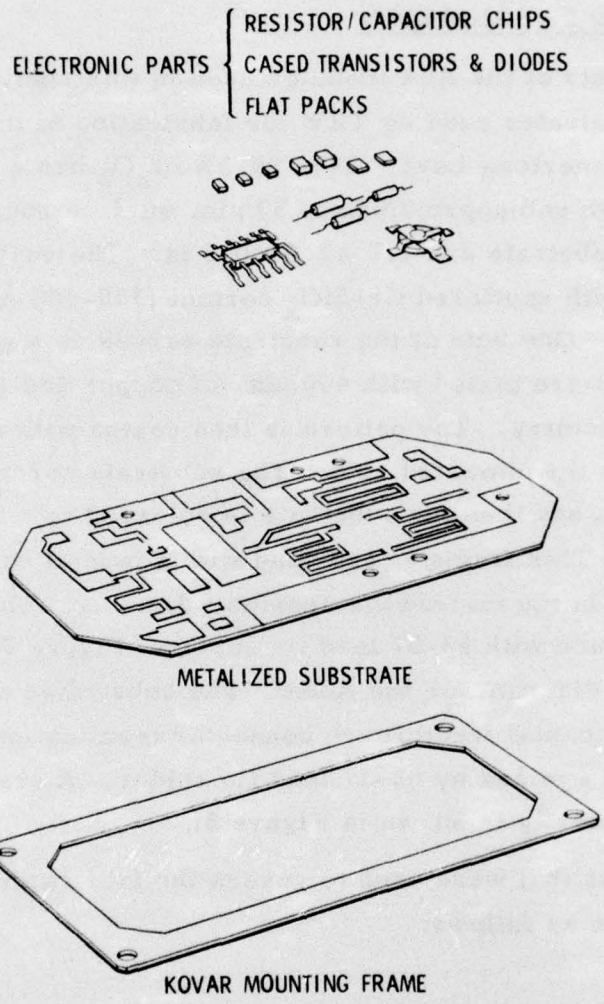

Figure 1. Alumina Substrate Assembly (ASA)

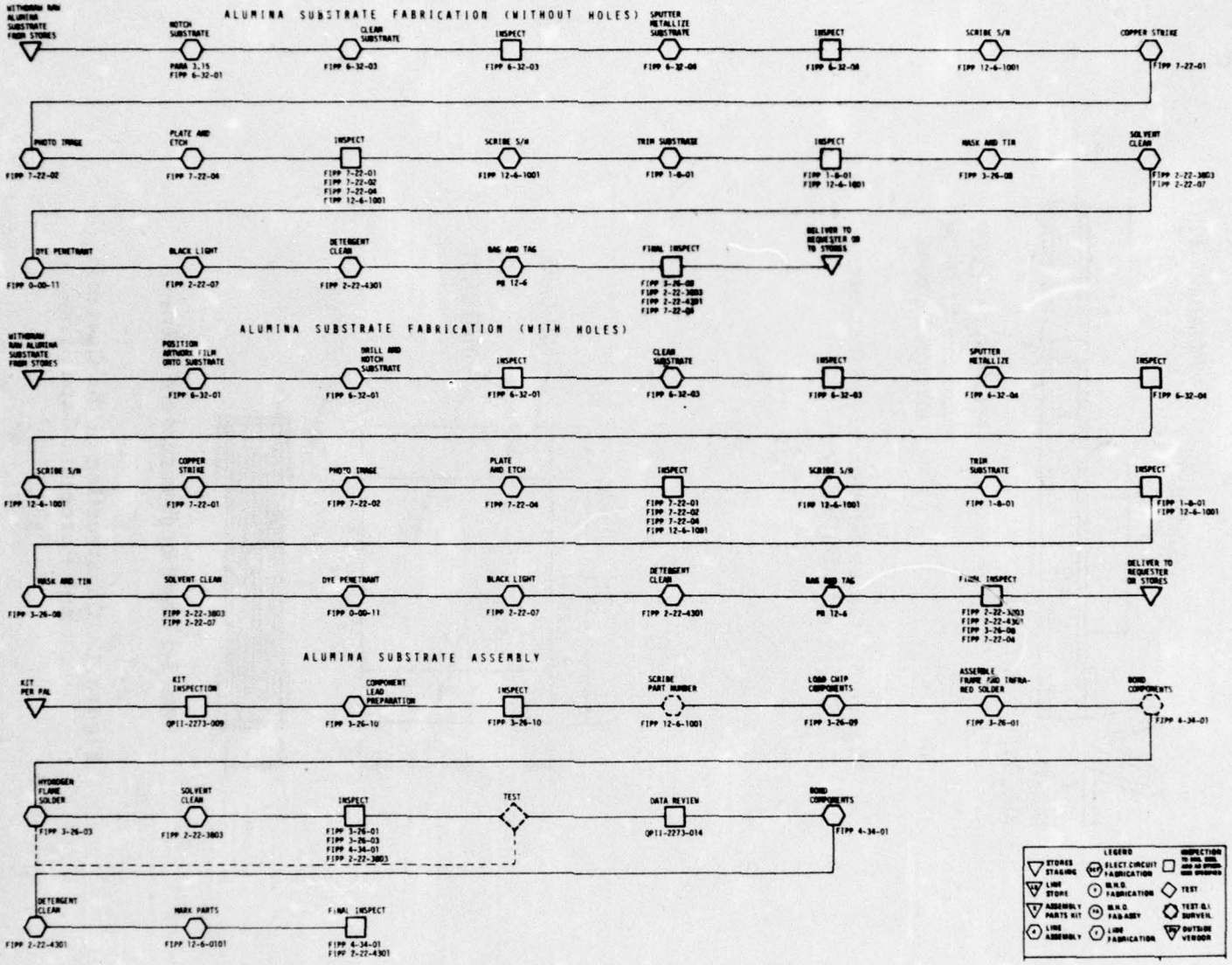

Figure 2. Manufacturing Flow Diagram for ASA

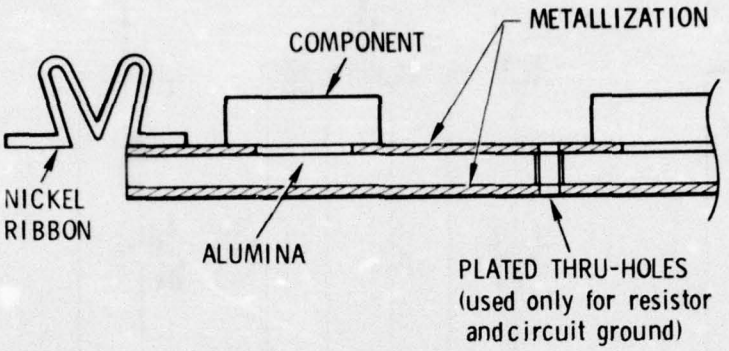

Figure 3. Cross Section of a Substrate with Butterfly

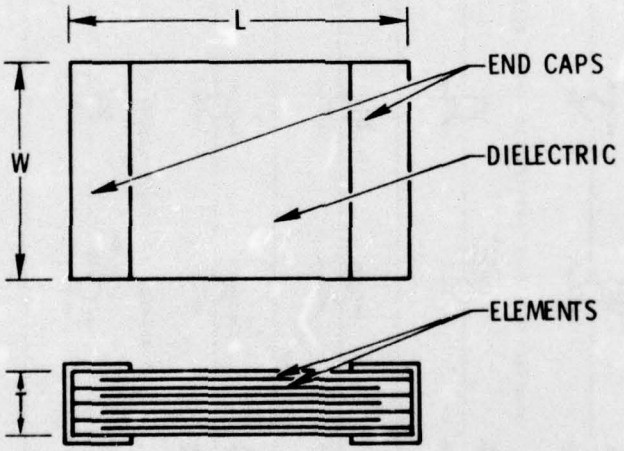

(Note: See Table 2 for dimensions and materials.)

Figure 4. Construction of the Ceramic and Porcelain Capacitors

Federal

QQ-S-571	Solder, Tin Alloy, Lead-Tin Alloy and Lead Alloy

TRW

MT3-74	Alumina, Unglazed, Substrate Grade
PR3-26	Assembly of Components and Kovar Frames to Alumina Substrates
PR6-32	Printed Wiring Boards, Alumina Substrate, Sputtered Metallization of
PR7-22	Printed Alumina Substrate Wiring Boards, Single and Double Sided, Fabrication of

The candidate components affixed to the ASA substrates were capacitors (both fixed and variable) thick film resistors, and inductors (both fixed and variable). The types of components are described in the following paragraphs.

1. CERAMIC CAPACITORS

The capacitors studied used either ceramic or porcelain dielectric. The ceramic or barium titanate capacitors have a high dielectric constant (K) that is optimized at 120°C. Various additives are normally employed to broaden the temperature of maximized K and to shift it toward 25°C. These additives are considered proprietary and vary with the capacitor types and suppliers. They include $SiTiO_3$, $CaZrO_3$, $BaZrO_3$, $CaTiO_3$, $MgTiO_3$, Nb_2O_5, and Ta_2O_5, and are generally considered to be "low" percentage.

The porcelain capacitors were included because of their very high Q (greater than 10,000 at 1 MHz). The composition of the porcelain was not given, but could be either electrical or steatite. Electrical porcelain generally consists of approximately 50% clay [$Al_2Si_2O_3(OH)_4$], 25% flint [SiO_2], and 25% feldspar ($KAlSi_3O_8$) before firing. Steatite porcelain is generally composed of approximately 90% talc [$Mg_3Si_4O_{10}(OH)$] plus 10% clay.

Both the ceramic and porcelain capacitors used for ASA were layered structures to attain high capacitance per unit volume as shown in Figure 4.

Capacitance dimensions and materials of the capacitors used in the study are listed in Table 2. Metallization of the end caps to establish continuity to the internal layers and the conductors of the substrate was accomplished using fired thick film conductors. Plated layers were included as barriers between the thick film and solder to inhibit dissolution of the fired metallization in the molten solder during assembly.

It should be noted that the number of layers together with the ceramic compositions determines the value of the capacitance. Therefore, the basic size as well as the capacitance (number of interlayered conductors) are variables and no single chip capacitor can be considered representative of all values and sizes used for the ASAs.

2. VARIABLE (TRIMMER) CAPACITORS

The variable (trimmer) capacitors illustrated in Figure 5 were manufactured by Johanson Manufacturing Company. The two electrical contacts of the capacitor were established on the cylindrical gold-plated metal base and a gold-plated Kovar strap. Because there were four different sizes available and only one unit was to be tested, the criterion used in selecting the capacitor was size; i.e., the largest physical size available was chosen.*

3. FILM CHIP RESISTORS

Thick film chip resistors (Types 1K011 and 1K007) were fabricated by two suppliers, Dale Electronics and Pyrofilm Corporation. Two sizes were available from both suppliers with approximately 265 resistive values. Of these, both sizes and four resistances were used in this study. Both suppliers used 96% alumina for the body of the chip, and fabrication consisted of screening the resistor and conductor inks onto an alumina substrate. They were then fired in several rows. After firing, each row was sawed or broken into strips.

*Originally, this capacitor was to be designated part No. 1A005-004V-001 (0.8-8.0 pF), but was changed to No. 1A005-002V-001 (0.6-4.5 pF) because of the unavailability of the former part.

Table 2. Details of Chip Capacitor Construction

Capacitor*	Capacitance	L, in.	W, in.	T, in.	Dielectric	Elements	End Caps
C1-C6	33 pF	0.070	0.055	0.055	Porcelain	Palladium	Pd-Ag-N_i-SN 60
C7-C10	270 pF	0.090	0.055	0.060	$BaTiO_3$ (NPO)	Pt, Pd, Au	Ag-Cu-SN 60
C11-C14	470 pF	0.075	0.045	0.060	$BaTiO_3$ (BX)	↓	↓
C15-C18	1500 pF	0.175	0.125	0.060	$BaTiO_3$ (NPO)		
C19-C22	1800 pF	0.175	0.125	0.060	$BaTiO_3$ (NPO)		
C23-C24	0.1 μF	0.095	0.055	0.060	$BaTiO_3$ (BX)		
C25-C31	1.0 μF	0.175	0.125	0.060	$BaTiO_3$ (BX)		

*C1-C6 – manufactured by American Technical Ceramics.
C7-C31 – manufactured by Union Carbide Corporation.

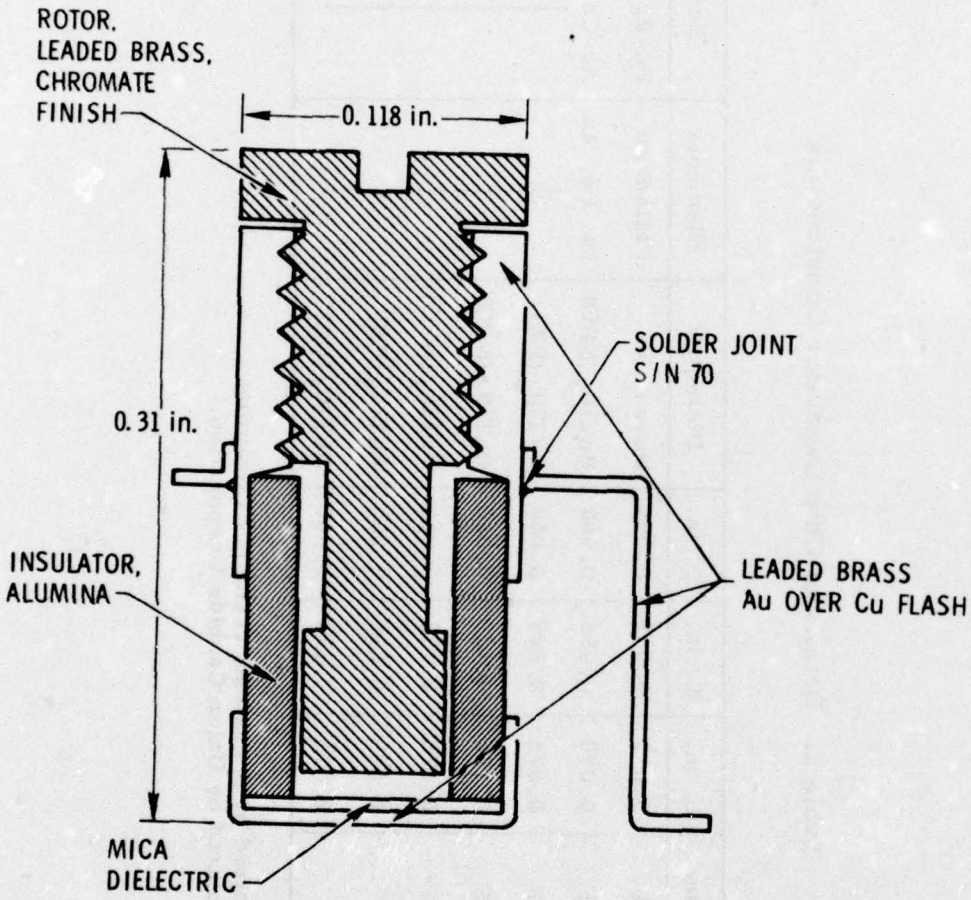

Figure 5. Construction of the Variable Capacitor

Two different methods were used to establish continuity between the resistor element and the bottom/end of the chip where the solder connection was made:

a. Dale Electronics used thick film ink. Initially, the strip was dipped into the ink, but other procedures were being considered.

b. Pyrofilm Corporation used vacuum-deposited nichrome overplated with nickel.

Dale broke the strips to yield the individual chip resistors while Pyrofilm diamond sawed the strip. Pyrofilm screened the resistor/metallization as discrete areas and, consequently, the diamond saw cut only alumina. Dale's resistor/metallization screening was continuous and fracture of the alumina resulted in a fracture through the resistor/metallization thick film.

Both Dale and Pyrofilm used air abrasion of the resistor element to obtain the desired resistance. Dale performed this process after the chips were separated from the strip, but it was done by Pyrofilm while the material was in the substrate configuration. Pyrofilm also screened a plastic material over the resistor element to provide stability. A cross section of a typical thick film resistor is shown in Figure 6.

4. INDUCTORS

Piconics, Incorporated manufactured the inductors, which consisted of polynylon insulated magnet wire that was wound on a mandrel. The wire ends were parallel-gap welded to substrate bonding pads, and the coil was conformally coated with epoxy and injection molded to its final form with glass fiber filled diallyl phthalate. The variable inductors also included a threaded slug within the coil mandrel. Cross-sectional drawings of the fixed and variable inductors are shown in Figures 7 and 8 respectively.

5. SUMMARY OF MODULE FABRICATION

In the design of the ASAs an attempt was made to include a wide variety of chip resistor, capacitor, and inductor case styles and physical sizes in a simple series/parallel network of elements with no specific function. In

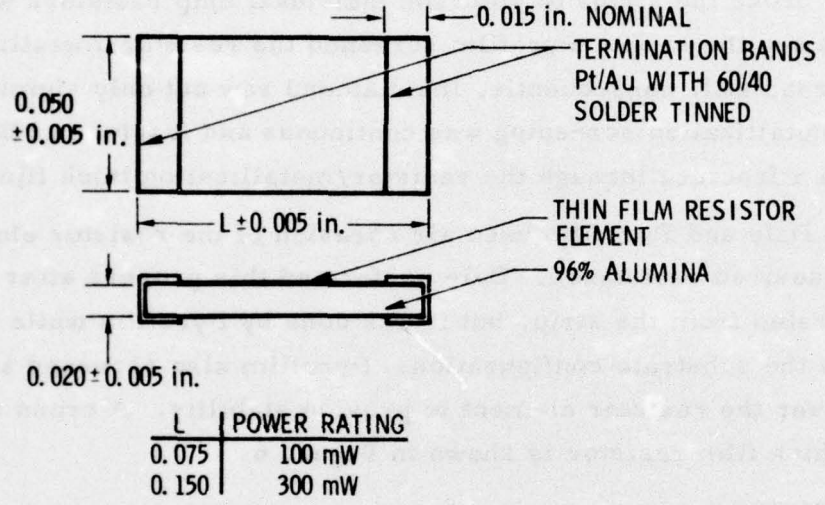

L	POWER RATING
0.075	100 mW
0.150	300 mW

Figure 6. Construction of the Thick Film Resistor

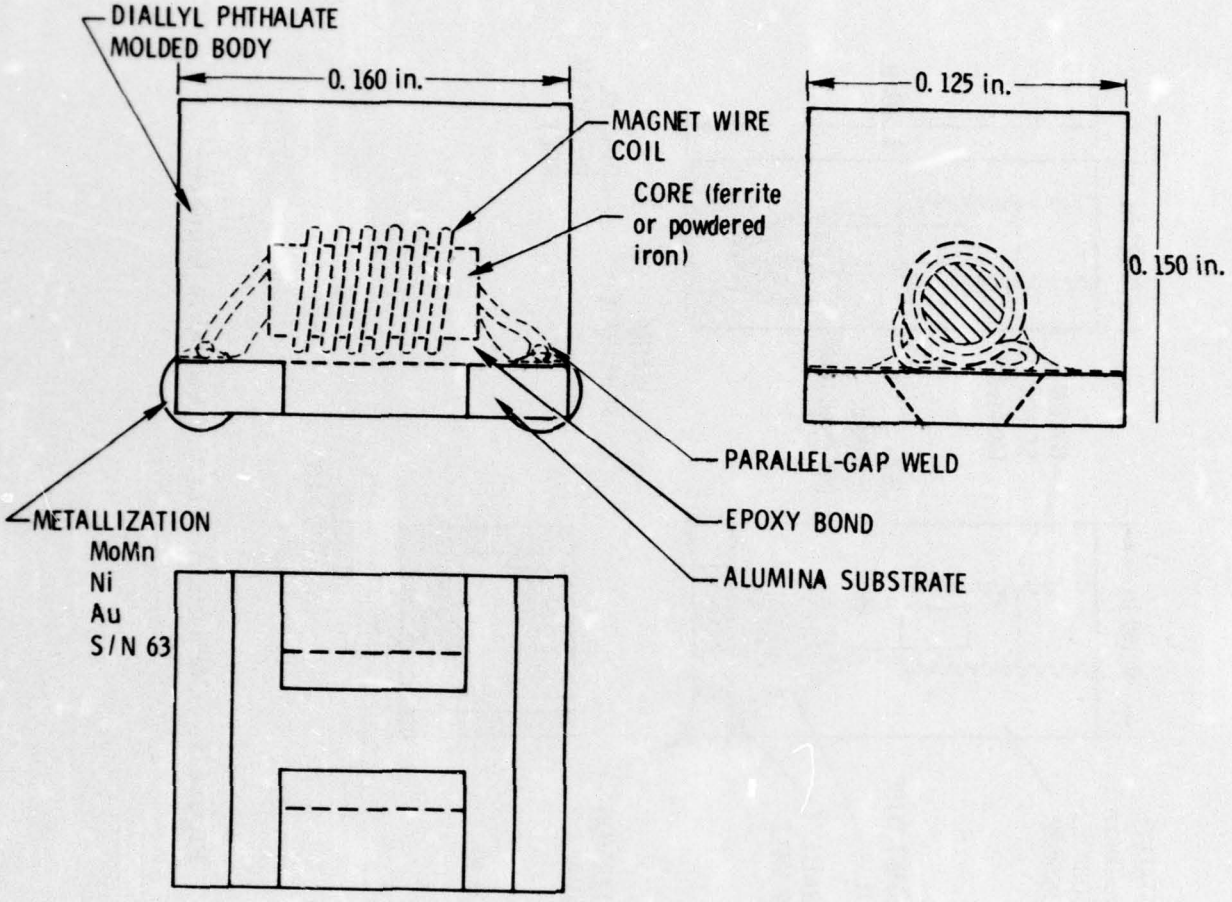

Figure 7. Construction of the Fixed Inductor

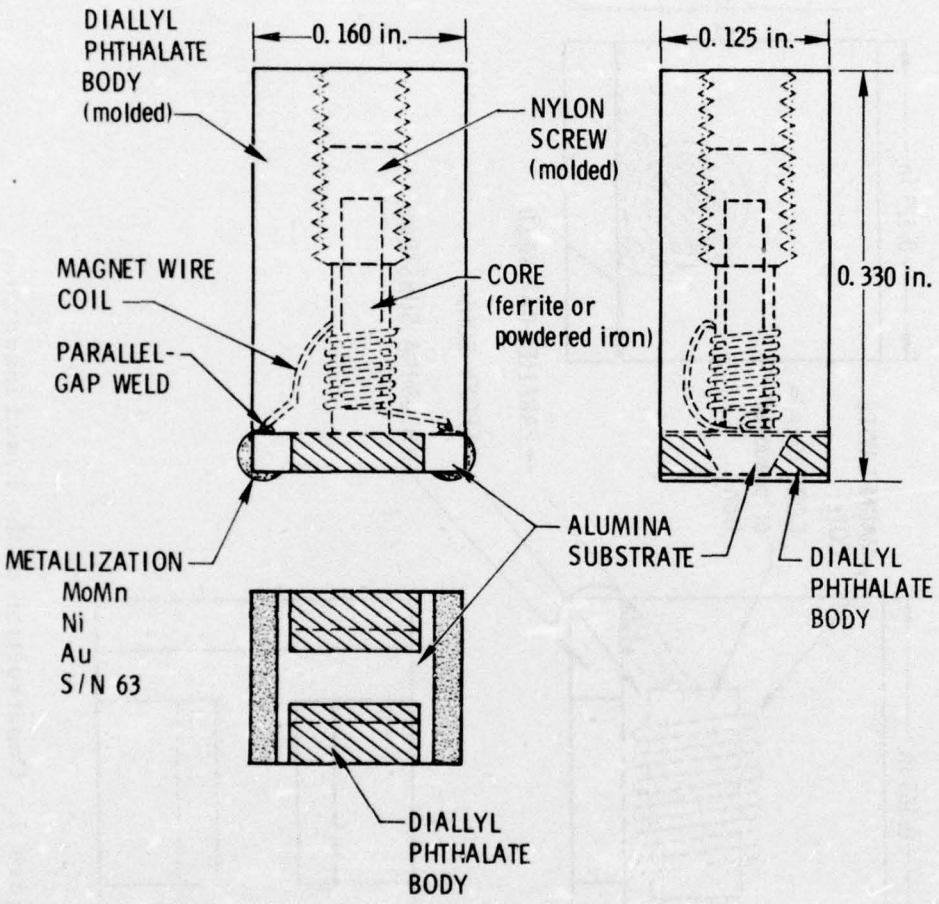

Figure 8. Construction of the Variable Inductor

addition, test probe pads were arranged in the substrate layout pattern around each element in such a manner that the parameters of each element could be sensed without compromising the primary functional current path on each substrate network. Four networks of 20 to 24 elements were provided on each of three identical test assemblies. The parts list for each network is given in Table 3.* For monitoring purposes, each ASA module was accessible for end-to-end transfer function measurements on each of the four networks. The three ASA modules that were fabricated are shown in Figures 9, 10, and 11.

The networks were designed so that during the environmental testing each network was excited with an ac signal at a carrier frequency in such a manner that an intermittent catastrophic parameter change on any individual network element would provide a detectable change in the magnitude of the output of the entire network. Of the four networks in each ASA module, networks 1, 2, and 3 are high pass resistance-capacitance (R/C) circuits, each with two identical sections in series. Network 4 is a low pass inductance-resistance (L/R) circuit, again with two identical sections in series. These networks are shown schematically in Figure 12.

B. TEST EQUIPMENT DESIGN

Test cables for the temperature cycling and vibration tests were on the order of 81 in. in length with a shunt capacitance on the order of 20 to 30 pF per foot of length. This shunt capacitance makes it imperative that buffer amplifiers be used to isolate the ASA network from the cable capacitances. Such isolation is particularly necessary when measuring the equivalent circuit capacitance and resistances for ASA networks 1 through 3. The inductance of each string of coils in ASA network 4 is approximately 4 μH with an impedance of 25 Ω at 1 MHz. Figure 13 is an illustration of the general test circuit for a channel.

---

*It should be emphasized that the identical networks on the two substrates in each module were connected in series. Thus the total part count for each circuit is two (2) times that for the network on a single substrate.

Table 3. Parts List for Each Substrate

				Quantity per Substrate
	Network 1			
C1-6	1A010-450X	Chip Capacitor, Fixed Porcelain	33 pF	6 ea.
C7-10	1A036-104X	Chip Capacitor, Fixed Ceramic	270 pF	4
R1-2	1K011-319X	Resistor, Chip, Film	82.0 kΩ	2
	Network 2			
C11-14	1A036-029X	Chip Capacitor, Fixed Ceramic	470 pF	4
C15-18	-158X	Chip Capacitor, Fixed Ceramic	1500	4
C19-22	-164X	Chip Capacitor, Fixed Ceramic	1800	4
R3-4	-302X	Resistor, Chip, Film	16.0	2
	Network 3			
C23-24	1A036-337X	Chip Capacitor, Fixed Ceramic	10,000 pF	2
C25-31	-349X	Chip Capacitor, Fixed Ceramic	100,000	7
R5	1K011-280X	Resistor, Chip, Film	2.0 kΩ	1
	Network 4			
L1	1R003-009X	Coil, Chip rf Fixed	0.68 μH	1
L2	-010X	Coil, Chip rf Fixed	1.0	1
L3	1R002-010X	Coil, Chip rf Variable	0.560-0.350	2
L4	-011X	Coil, Chip rf Variable	0.860-0.540	1
L5	-211X	Coil, Chip rf Variable	0.860-0.570	1
R6-7	1K007-065X	Resistor, Chip, Film	470.0 Ω	2
		Attached but Not Connected in a Network		
C9	1A005-002V	Capacitor, Var, Trimmer	0.6-4.5 pf	

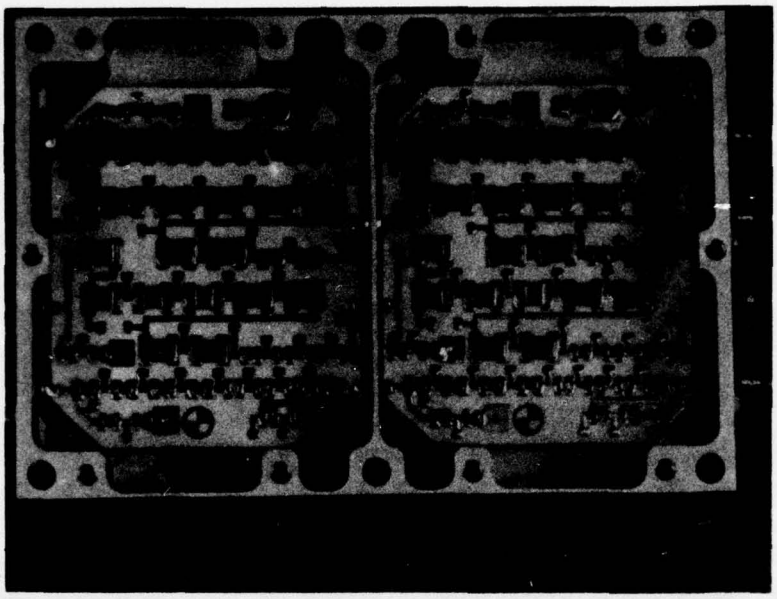

Figure 9. ASA Module S/N 001, Internal View. (Substrate No. 1 is on the left. The variable capacitor may be seen at the upper right of each substrate. The various circuit networks may be seen with No. 4 at the top and No. 1 at the bottom of the substrate.)

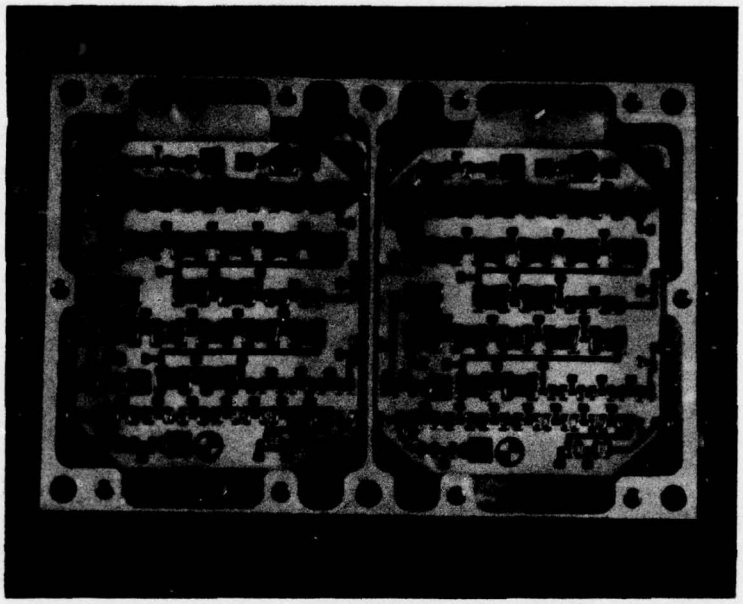

Figure 10. ASA Module S/N 002, Internal View. (Substrate No. 1 is on the left. The variable capacitor may be seen at the upper right of each substrate. The various circuit networks may be seen with No. 4 at the top and No. 1 at the bottom of the substrate.)

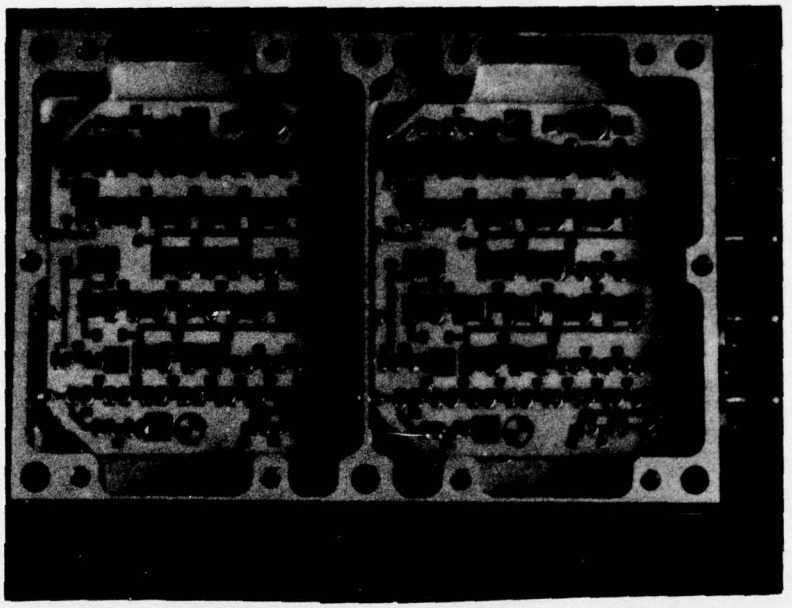

Figure 11. ASA Module S/N 003, Internal View. (Substrate No. 1 is on the left. The variable capacitor may be seen at the upper right of each substrate. The various circuit networks may be seen with No. 4 at the top and No. 1 at the bottom of the substrate.)

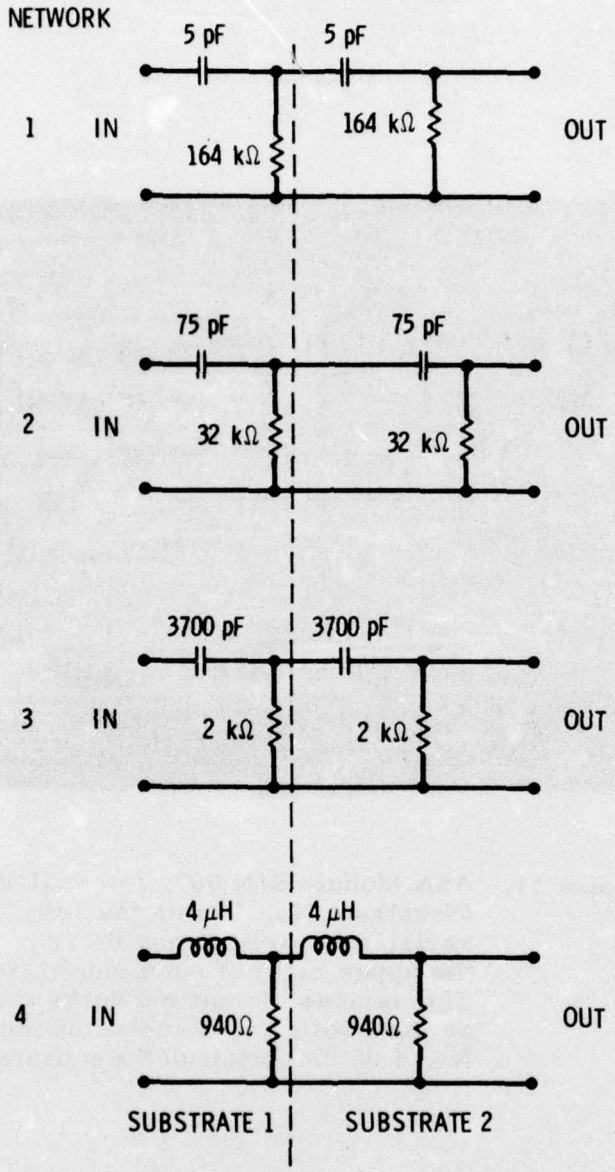

Figure 12. Equivalent Circuits for One ASA Module. (The dotted line separates equivalent circuits for the two substrates.)

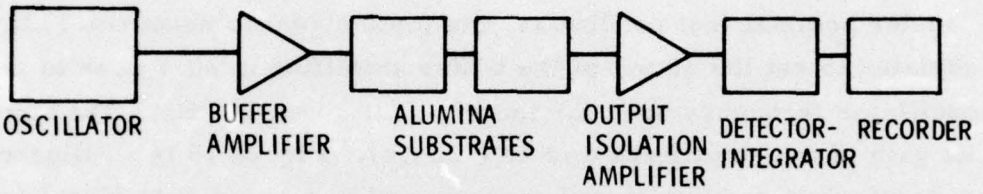

Figure 13. Block Diagram of Test Circuit for One Network

Figure 14 is a schematic of the wideband ac buffer amplifier made up from a commercial grade (393 grade) μA 715 operational amplifier integrated circuit and a complementary emitter follower. This amplifier design was used both for the input buffer between the test oscillator and each network under test and as an output isolation amplifier.

The amplifier input impedance was greater than 1 MΩ in parallel with the shunt capacitance of the input cable. Cable length between the amplifier and the network under test was kept to a minimum, resulting in an expected input/output shunt capacitance of 5 to 10 pF.

Under nominal test conditions, the input signal to networks 1, 2, and 3 was adjusted to set the output of the buffer amplifier to 20 V peak to peak. The oscillator frequency used for these circuits was 50 kHz. The nominal voltage gain of the amplifiers was 40 (+32 dB). Figure 15 is an illustration of the simple detector-integrator circuit used to develop a dc signal proportional to the magnitude of the ac output of the network under test. This detector circuit is driven by the output buffer amplifier described above. For network 4, an additional dc bridge circuit is included in the input buffer/amplifier to monitor resistor as well as inductor performance. This circuit, shown in Figure 16, is tuned to the series resonance of the inductors under test (about 608 kHz).

C. TEST PLAN

Each ASA module was opened and probed, with initial acceptance at Aerospace to establish electrical parameter values on each element in the installed (mounted) condition.

Following acceptance, the tests performed by Aerospace on the modules included thermal cycling, random vibration, shock, and destructive physical analysis (DPA). These were accomplished in two groups designated Phase I and Phase II; the Phase I tests were performed at three temperatures while Phase II tests were only at room temperature. Both the type of test and the sequence followed is given in Table 4.

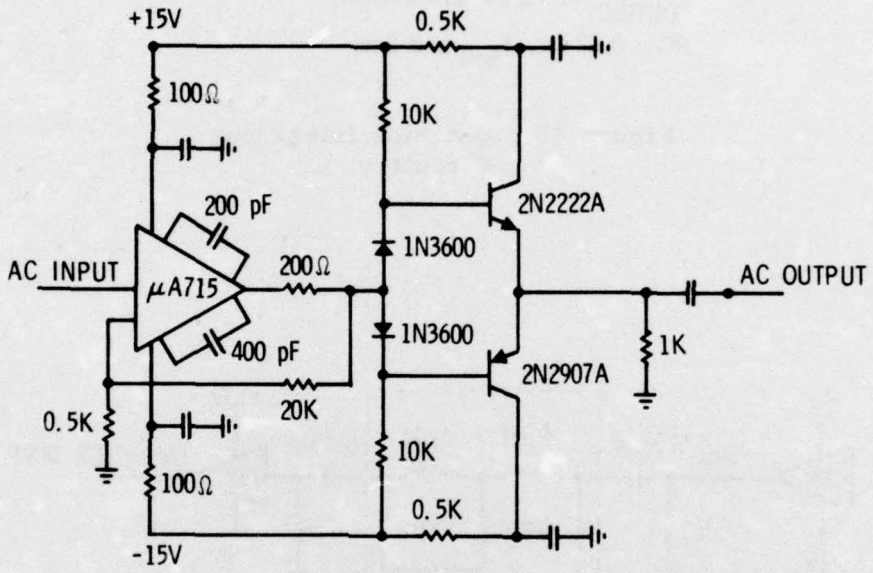

Note: All capacitors = 0.1 μF unless otherwise specified.

Figure 14. Circuitry of a Buffer/Output Isolation Amplifier

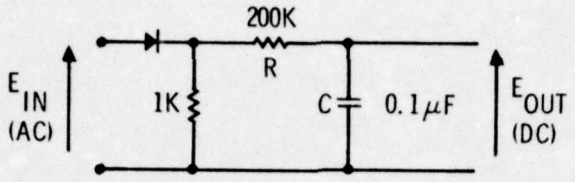

$E_{IN(AC)} \approx 20V$ PEAK-TO-PEAK NOMINAL

$E_{OUT(DC)} \approx +3.2V$ dc NOMINAL

RC = 0.02 sec, $F_{3dB} \approx 8.0$ Hz

Figure 15. Detector Integrator Circuitry

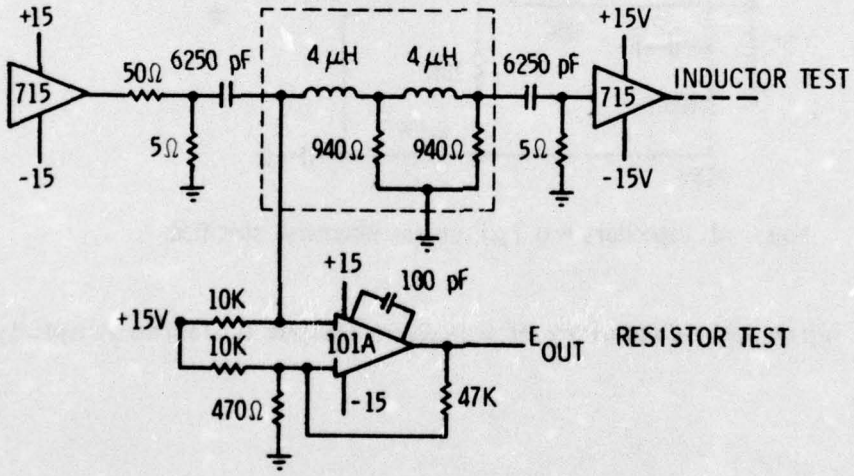

Figure 16. Resistance Monitoring Circuit for Inductor (No. 4) Network. (In addition to the inductor network, shown enclosed by the dotted line, the buffer and output isolation amplifiers are shown for completeness. The monitoring circuit for resistance is connected at the output of the buffer/amplifier.)

Table 4. Sequential Test Plan

Test Symbol	Test Description	Temp (°C)	Elec. Monitor	Module No. 001	002	003
PHASE I						
A1	Random Vibration - 1.0 g^2/Hz, 6 min,* three axes	room temp	X	X	X	X
A2	Random Vibration - 0.3 g^2/Hz, 6 min, three axes	-35	X	X	X	X
A3	Random Vibration - 0.3 g^2/Hz, 6 min, three axes	+60	X	X	X	X
B1	Shock - 2500 g peak,** three axes	room temp	X	X	X	X
B2	Shock - 2500 g peak, three axes	-35	X	X	X	X
B3	Shock - 2500 g peak, three axes	+60	X	X	X	X
C	Thermal Cycle (200 cycles)	-46 to +60	X	X	X	X
D	Thermal Cycle (800 cycles)	-50 to +100	X	X	X	X
PHASE II						
E	Random Vibration - 1.0 g^2/Hz, 6 min, vertical axis	room temp			X	
F	Shock - 2500 g peak, lateral axis	room temp			X	
G1	Thermal Cycle (5 cycles)	-65 to +125		X		
G2	Thermal Cycle (5 cycles)	-80 to +150		X		
H	DPA (side A only)					X

*6 min per axis.

**1 shock each axis.

Since the facilities were not available at Aerospace, the random vibration and shock tests for both Phase I and II were accomplished at the Approved Engineering Test Laboratories (AETL).* Thermal cycling and the DPA were performed in the Failure Analysis Laboratory at The Aerospace Corporation.

D. VIBRATION TEST SETUP

The vibration test fixture was calibrated by affixing it to the vibration exciter without ASA modules mounted and subjecting it to evaluation over the frequency range of 50 to 2000 Hz at an applied acceleration of 5.0 g peak. During the fixture evaluation, the outputs of the control and response accelerometers, mounted as illustrated in Figure 17, were recorded on X-Y plots. A typical power spectral density (PSD) plot is shown in Figure 18. The bare fixture was then subjected to fixture evaluation in each of the three major orthogonal axes over the frequency range of 20 to 2000 Hz using random vibration at the following intensities:

Frequency (Hz)	Intensity
20 - 100	6.0 dB/octave rise
100 - 1000	1.0 g^2/Hz
1000 - 2000	6.0 dB/octave roll-off
Overall Acceleration	36.0 g rms (root mean square)

The X-Y plots for Phases I and II are contained in AETL reports Nos. 5330 to 2134 (3 April 1975) and 5330 to 2716 (23 Jan 1976), respectively. These reports are presented here in abbreviated form as Appendixes A and B. The PSD plots obtained during fixture evaluation are contained in the referenced reports.

In Phase I, each module was installed in the test fixture as shown in Figure 17 and mounted on the vibration exciter. The module was then

*Located at 5320 West 104th Street, Los Angeles, California 90045.

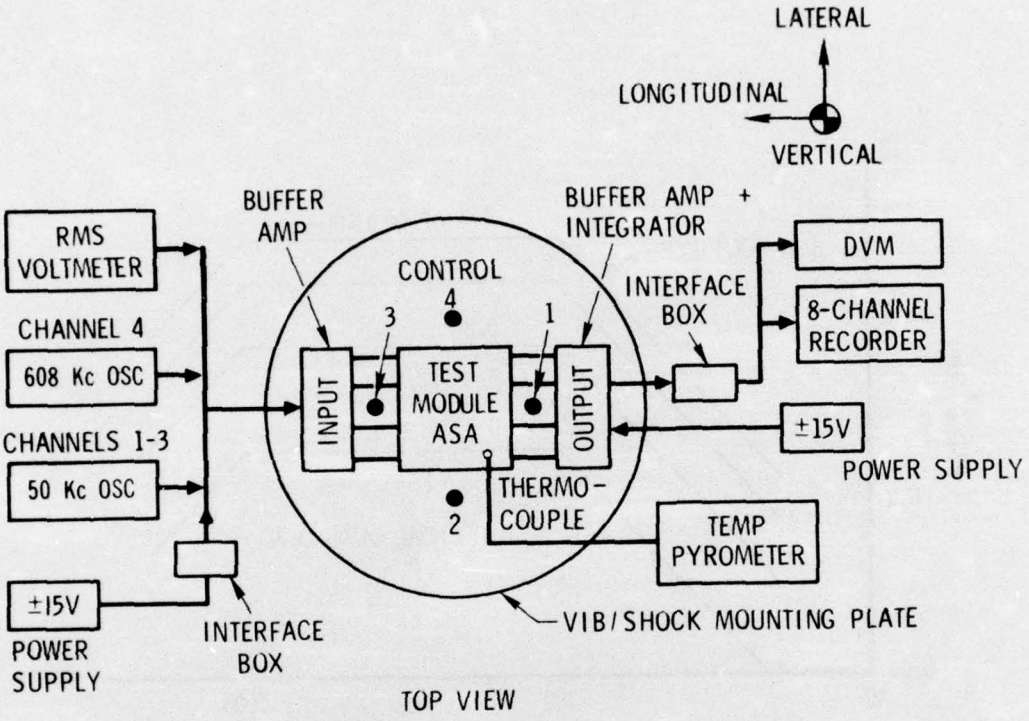

(Note: Control and response accelerometers were always mounted in the direction of vibration.)

Figure 17. Arrangement of Module and Amplifier on Fixture for Vibration Test. (The locations of the response accelerometers are indicated by the Nos. 1 through 3. The control accelerometer is in location 4.

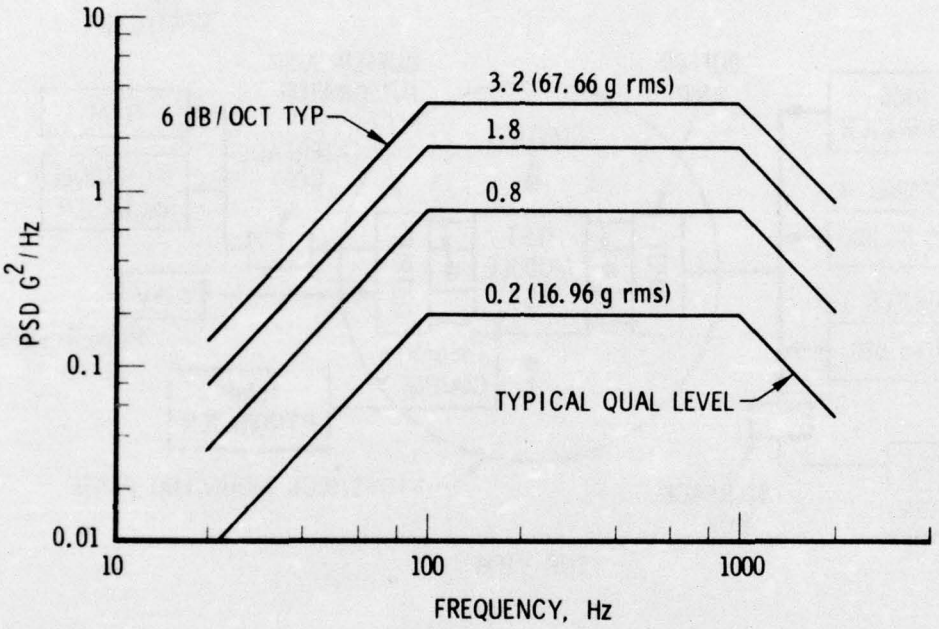

Figure 18. Typical Power Spectral Density Plot for Vibration Test

subjected to six (6) min of random vibration in each of the three major orthogonal axes. A frequency range was used of 20 to 2000 Hz at the intensities listed above for the 36.0 g (rms) level at room temperature. Tests were also performed at -35°C and +60°C. The test arrangement is shown in Figure 19 and the specific instruments used are described in the AETL test reports. During vibration testing, the modules were monitored electrically. This test arrangement is shown in Figure 17. In Phase II, module S/N 002 was subjected to six (6) min of random vibration in the vertical axis at room temperature. Electrical monitoring was performed before and after, but not during, this test. Visual examination followed testing in each axis.

E. PYROTECHNIC SHOCK TEST

The pyrotechnic shock test was also performed at AETL. For this test, each module was installed on a test fixture that was then affixed to the vibration exciter as shown in Figure 20. In the Phase I testing, the exciter was programmed to give one synthesized shock pulse in each of the three major orthogonal axes for each module at room temperature. This pulse had an amplitude of 2500 g with a maximum frequency of 10,000 Hz (see Figure 21). These tests were also performed on each module at -35°C and +60°C. Visual examination followed testing in each direction at each temperature.

In Phase II testing following the random vibration test, module S/N 002 was subjected to one (1) 2500 g peak shock, as described above, in the lateral axis only and only at room temperature. Electrical testing was performed before and after, but not during, this shock test.

F. THERMAL CYCLING TESTS

Thermal cycling testing of the modules was performed using the apparatus shown schematically in Figure 22. The equipment used for these tests is listed in Table 5.

It may be noted from Figure 23, which shows the arrangement of the modules in the environmental chamber, that the Aerospace-constructed buffer

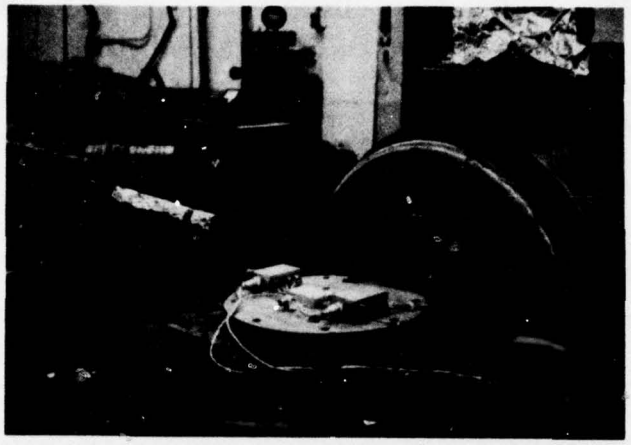

Figure 19. Fixture for Vibration Test with Module and Amplifiers in Place

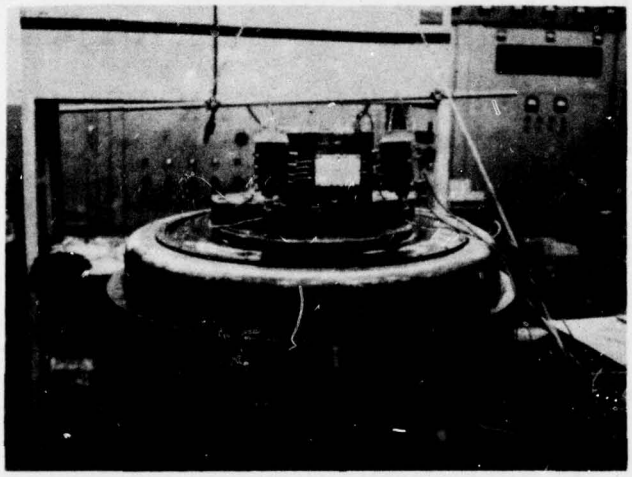

Figure 20. Fixture for Pyrotechnic Shock Test

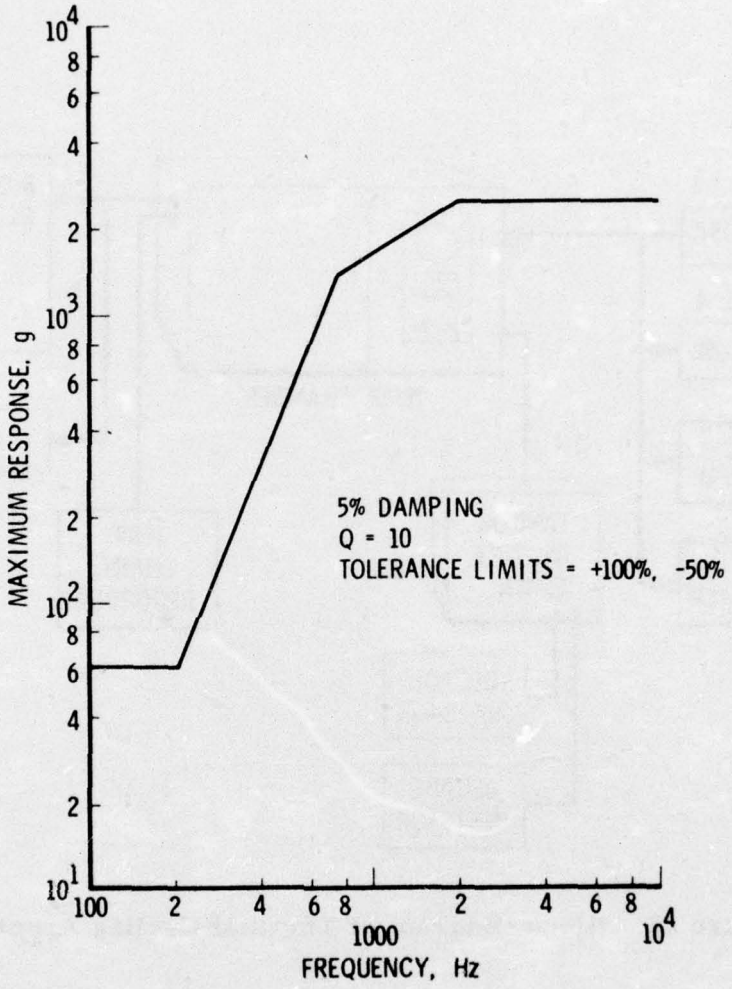

Figure 21. Typical X-Y Plot for Pyrotechnic Shock Tests

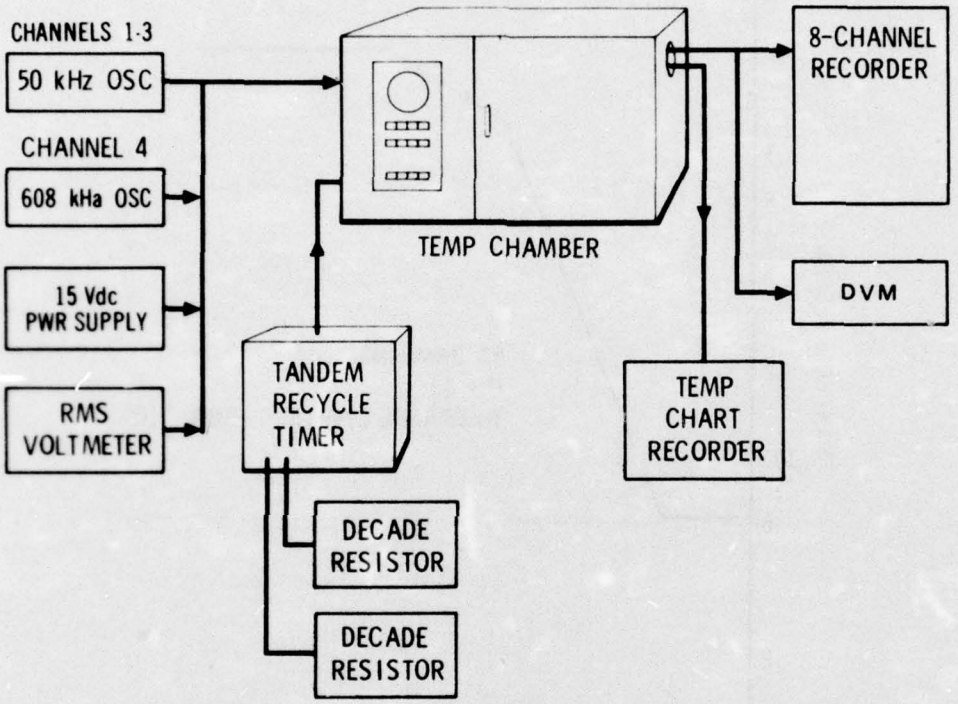

Figure 22. Block Diagram of Thermal Cycling Apparatus

Table 5. Equipment Utilized in Thermal Cycling Tests

Item	Manufacturer	Model
Temperature Cycle Chamber	Associated Environmental Systems	SK 2101
8-Channel Recorder	Hewlett Packard/Sanborn	7709-09A
50-kHz Oscillator	General Radio	1164-A
Digital Voltmeter (DVM)	Hewlett Packard	5327B
Root Mean Square (rms) Voltmeter	Hewlett Packard	403B
Power Supply	Kepco Hewlett Packard/Harrison	ABC-15-1 6200B
608-kHz Oscillator	Hewlett Packard	3320B
Tandem Recycle Timer	Industrial Timer Corp.	Type A
Decade Resistors (2)	General Radio	1432N
Temperature Chart Recorder	Leeds Northrup	Speedomax H

amplifiers were also subject to the test cycling. This approach was necessary to minimize the effects of cable capacitance. The recording of data from this test required eight channels as shown in Figure 24. The three modules were subjected to 200 temperature cycles ranging from -46°C to +60°C followed by 800 cycles from -50°C to +100°C. The frequency of these cyclic tests was 1 cycle per hour (CPH) and 0.5 CPH respectively. The modules were monitored continuously.

During Phase II, module S/N 001 was further subjected to an additional 5 cycles from -65°C to +125°C followed by 5 cycles from -80°C to +150°C. The frequency of these cyclic tests was 0.4 CPH. The module was not monitored during these tests.

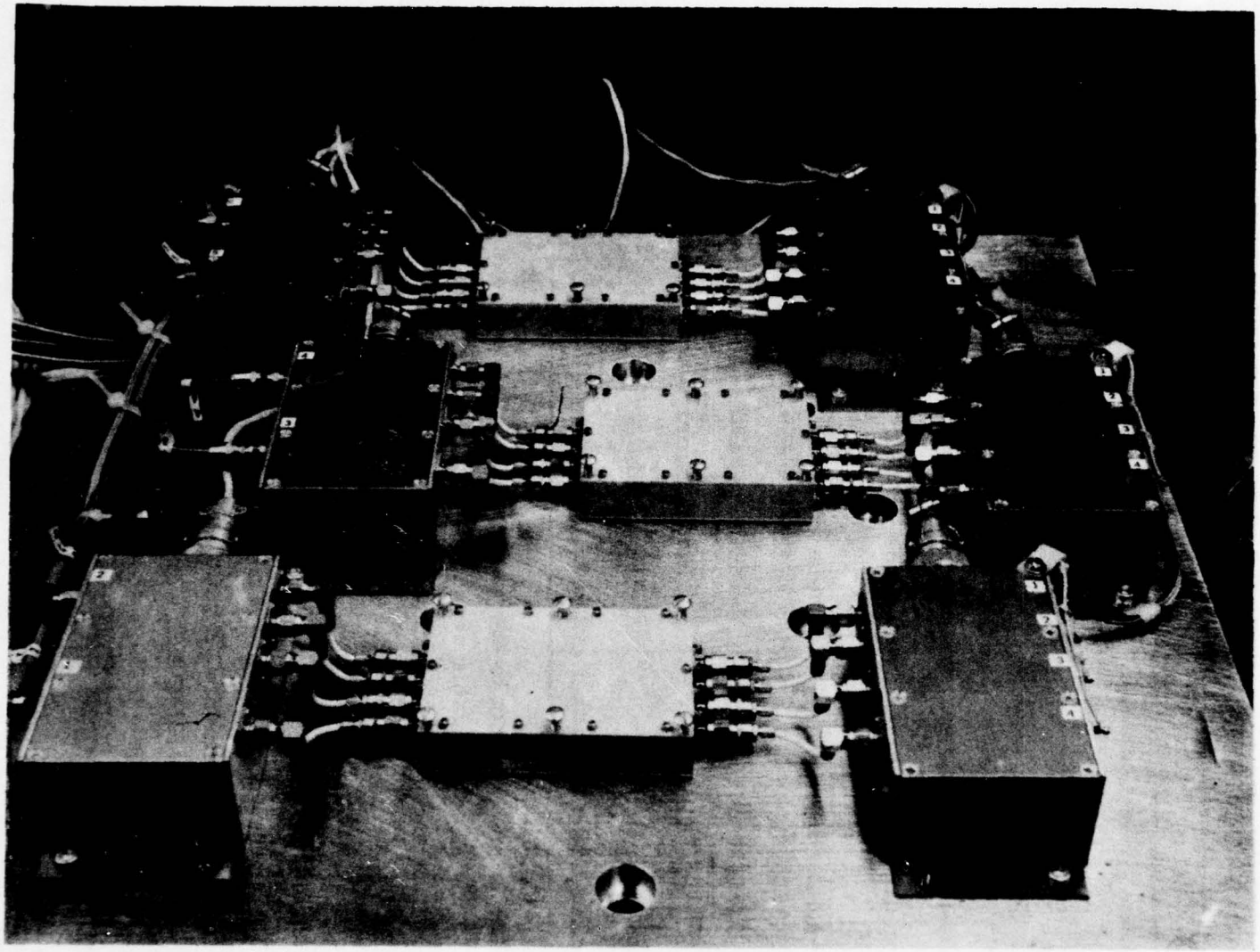

Figure 23. Arrangement of Modules and Amplifiers in Thermal Cycling Apparatus. (The ASA modules are located in the center of the apparatus with the buffer and isolation amplifiers on either side.)

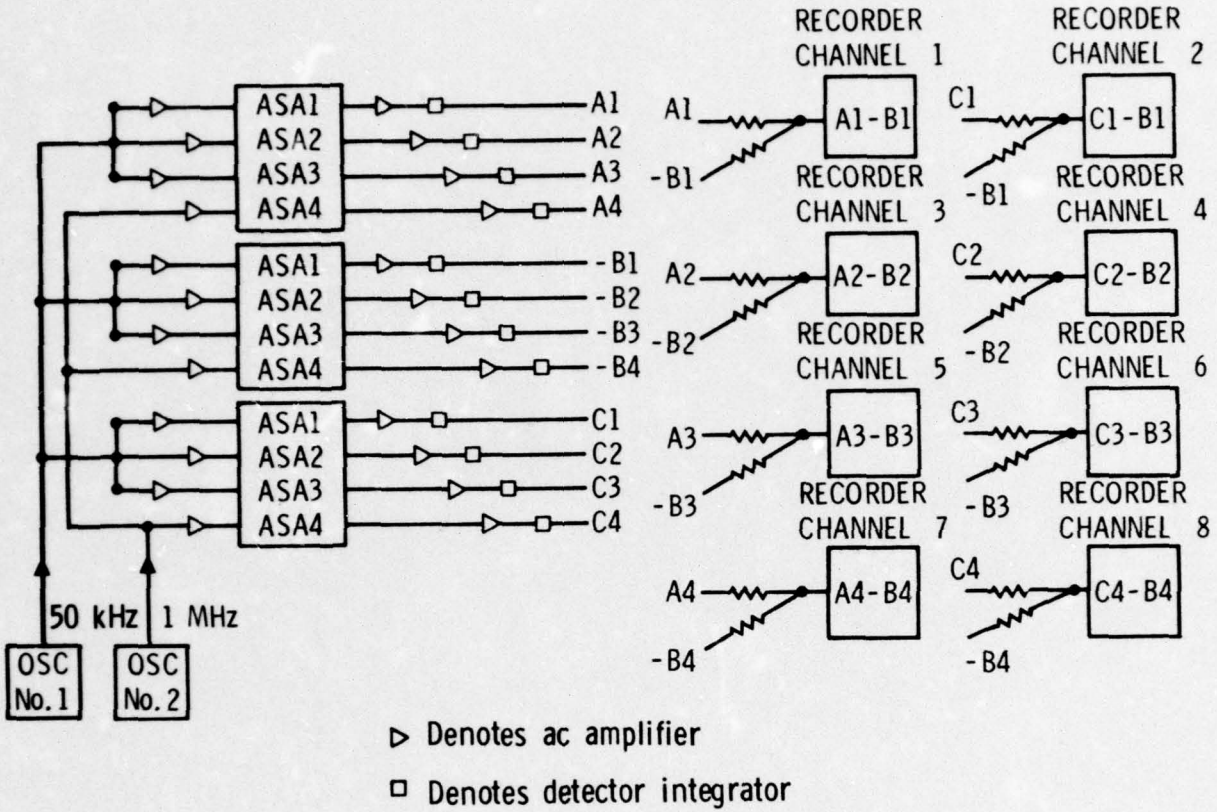

Figure 24. Schematic of Arrangement for Recording Data from Thermal Test

III. RESULTS

The modules were opened for examination and/or probing at each failure and after the 800 cycle and Phase II experiments for modules 001 and 002. The general condition of the substrates was found to be good. The solder fillets at the components showed extensive mechanical work and some cracking caused by the differential thermal expansion between the part and the substrate. However, it should be emphasized that no failures resulted from these effects. The failures observed were due mainly to components and are described in the following paragraphs.

The capacitor network 3 in module 003 exhibited intermittent noise during the vibration and shock testing. The components exhibited minor noise (15 mV) during Z-axis vibration at room temperature. This noise increased to 50 mV during z-axis vibration at test temperature extremes (-35°C and +60°C). The noise continued in the Z axis, but was not observed in the Y axis. During shock testing (2500 g) the noise increased to approximately 800 mV, and erratic readings were noted during the 30-min recovery period. The capacitor network 3 performed without incident during the subsequent 200 thermal cycles from -46°C to +60°C; however, it failed open shortly after commencing the 800 temperature cycles from -50°C to +100°C. Upon opening the module, a crack was observed across the center of C26, a 100,000 pF ceramic capacitor. (See Figure 25.) After removal of the capacitor by TRW, the crack could be seen on all four sides of the part. The failure analysis on C26 performed by TRW (see Appendix C) concluded that the cause of the failure was unknown. They had observed similar cracks resulting from thermal shock, but had no indication that vibration or shock testing (to 10,000 g) caused this failure mode. TRW speculated that a combination of thermal shock and vibration or mechanical shock could induce the defect.

The two pads for C26 were jumpered and testing was resumed. Two more capacitors in network 3 in module 003 exhibited failures during the 800 thermal

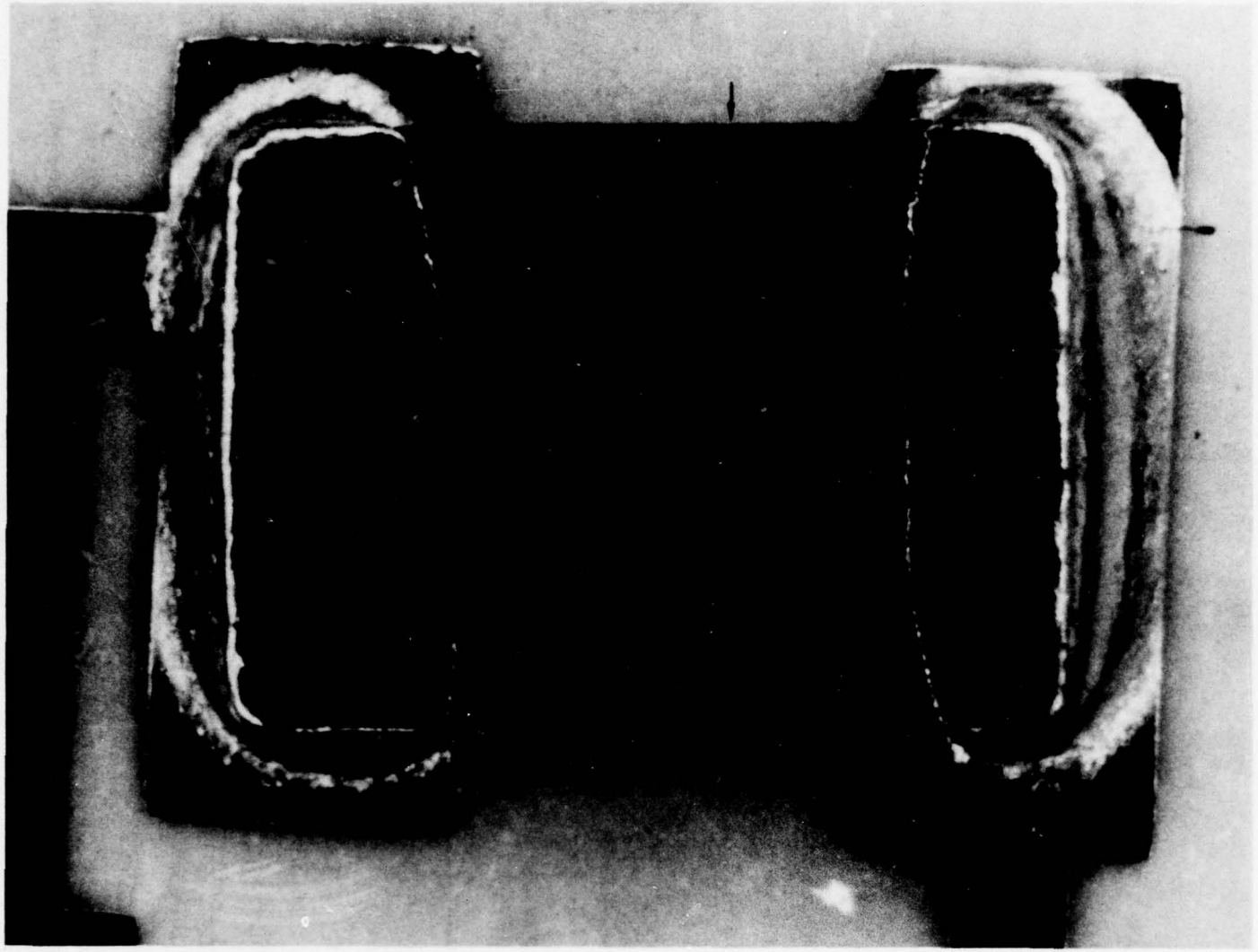

Figure 25. Photomicrograph of Failed Capacitor C26. (The arrows show the position of the crack that goes through the body of the capacitor.)

cycles ranging from -50°C to +100°C. Capacitor C23 (10,000 pF, ceramic) was intermittent and finally failed open. Capacitor C24 (10,000 pF, ceramic) was observed in post-test measurement to have changed values. Since module 003 underwent no Phase II testing, the examination of capacitors C23 and C24 was accomplished in the final cross sectioning of the module at The Aerospace Corporation. Figures 26(a) and (b) are scanning electron microscope (SEM) photos of the end cap areas of C23. Cracks originate at about the edge of the metallization, both top and bottom. These cracks extend under the end cap for some distance and are then joined by a crack that is roughly parallel to the end of the capacitor. It is evident that the open was caused by the crack which completely traverses the ceramic body. Other minor cracks are also evident in the end cap area, and voids are present in the end cap metallization. Figures 27(a) and (b) are SEM photomicrographs of the end cap regions of C24. Voids can be seen in the end cap metallization and could easily explain the observed intermittency.

Capacitors C25 (100,000 pF, ceramic) and C22 (1800 pF, ceramic) were also examined in cross section. These are shown in Figures 28(a) and (b) and Figures 29(a) and (b) respectively. These capacitors exhibit few voids in the end cap metallization and only inconsequential cracking of the ceramic.

Changes of about 10% were noted in the combined capacitance of network 1 in modules 001 and 002 after the vibration, shock, and 200 thermal cycle tests. No detailed examination was made to determine the source of this change.

The remaining part failures all occurred with the Piconics variable inductors. The first of these failures occurred in module 003 after 71 of the 200 temperature cycles (-46°C to +60°C). At the end of the 200 temperature cycles, the module was returned to TRW for failure analysis of the part(s). This failure analysis is given in Appendix D. At that time, it was determined that L6 of substrate 1 was "open" and that L6 of substrate 2 was "intermittent." The report concluded that the failures occurred as a result of cracks in the coil wire at the weld to the wrap-around connections. Since the crack showed

(a)

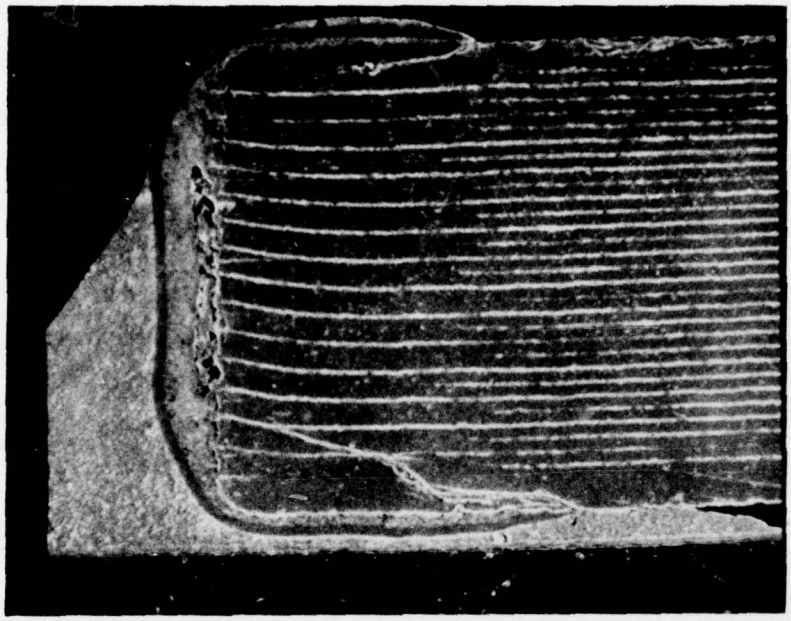

(b)

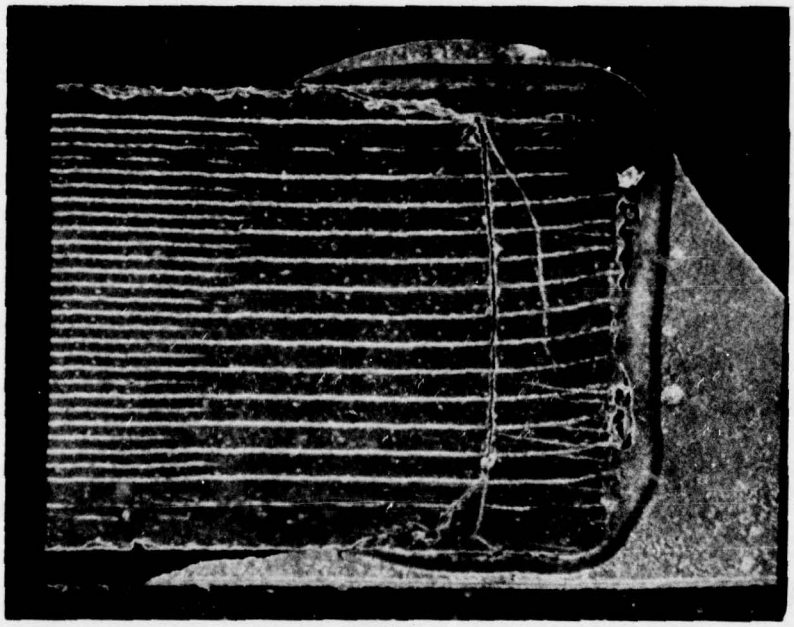

Figure 26. Scanning Electron Micrograph of the End Cap Areas of Capacitor C23 in Cross Section. (It should be emphasized that the major portion of the capacitor exhibited no cracking. Extensive cracking may be seen to originate at the ends of the end caps and radiate through the ceramic toward the end of this BX-type capacitor. The crack that is parallel to the end cap may be seen clearly in b.)

(a)

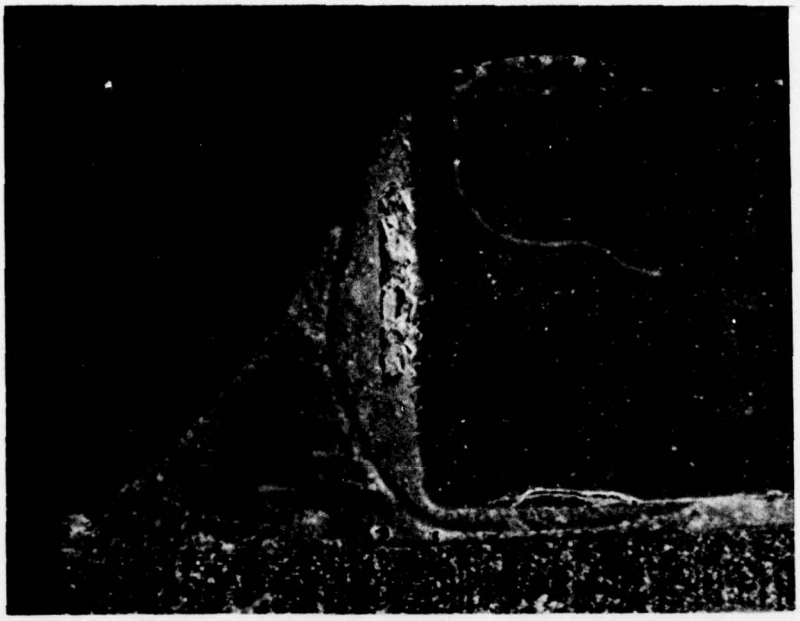

(b)

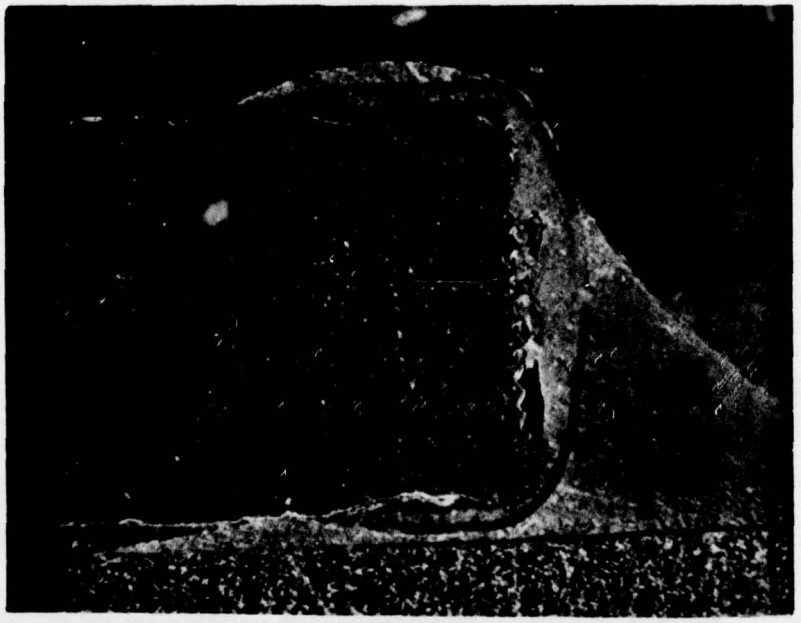

Figure 27. Scanning Electron Micrograph of the End Cap Areas of Capacitor C24. (In this BX-type capacitor no damage was observed except in the end cap areas where there was minor cracking of the ceramic and voids in the end cap metallization.)

(a)

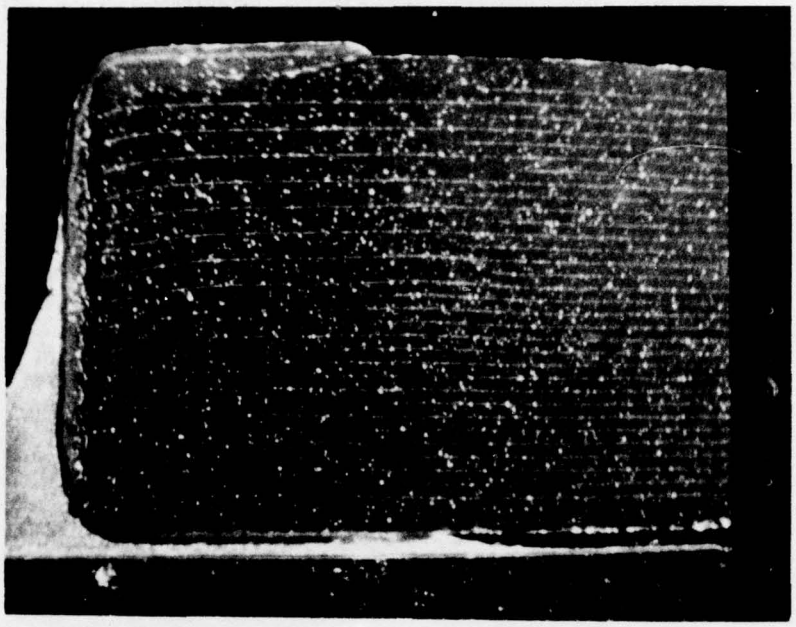

(b)

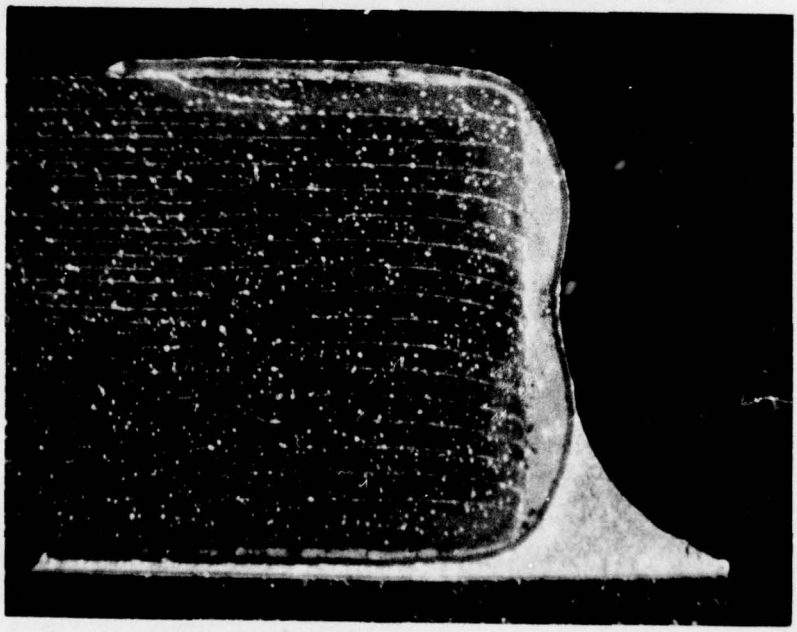

Figure 28. Scanning Electron Micrograph of the End Cap Areas of Capacitor C25 in Cross Section. (Little damage was observed in this BX-type capacitor except for very minor cracking of the ceramic in the end cap area.)

(a)

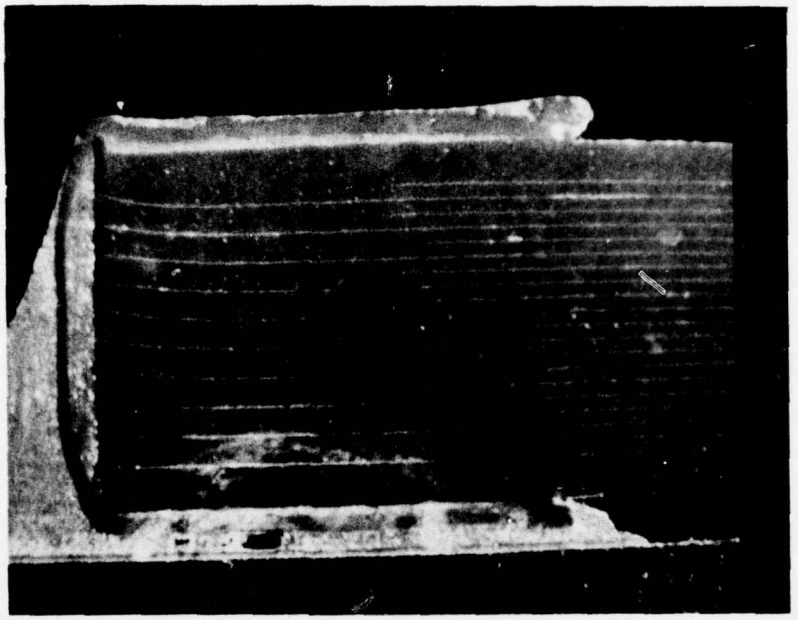

(b)

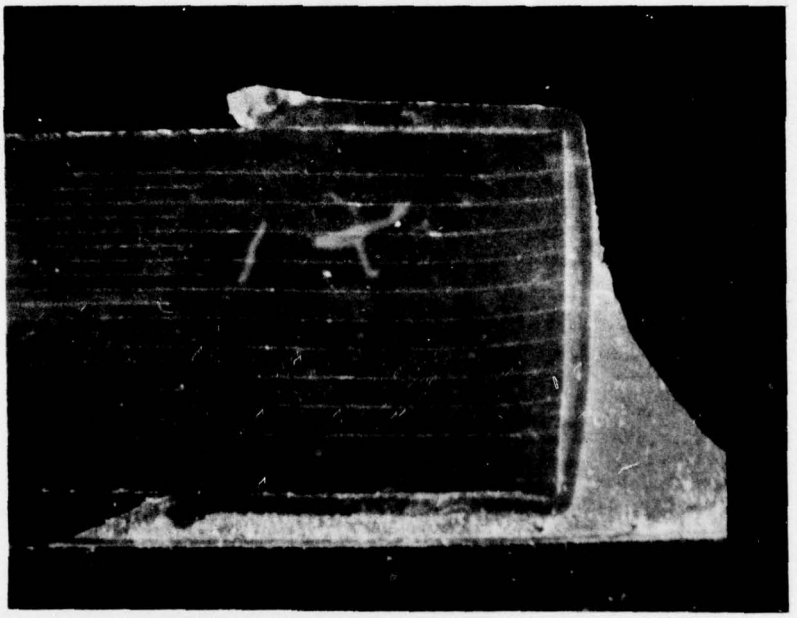

Figure 29. Scanning Electron Micrograph of the End Cap Areas of Capacitor C22 in Cross Section. (No damage was evident in the cross section of this NPO-type capacitor.)

evidence of being filled with epoxy, it was concluded that the initial condition resulted during device assembly. The ultimate failure was thought to have been caused by the complete separation of the wire as a result of the stress imposed by differences in the thermal coefficient of expansion of the materials used in construction of the component. It should be emphasized at this point that the portion of the inductor that was in contact with the ASA substrate was itself alumina and, thus, it is extremely unlikely that there could be thermal expansion stresses set up between the substrate and the part that could cause the failures. As a result of these failures, the remaining L6 inductors were bypassed with hard wire at the 108th cycle of the 800 temperature cycles. These inductors were not removed. At the 411th of the 800 temperature cycles, L5 of substrate 2 of module 003 failed open. This part was removed by TRW and a hard wire bypass installed. This inductor was not subjected to failure analysis.

One failure, detected after the Phase II vibration and shock test of module 002, consisted of a broken butterfly interconnect from substrate 1 to J8. This failure was attributed to a loose tiedown machine screw at the corner of the substrate, which permitted vibration with subsequent fatigue and failure of the butterfly. Figure 30 is a scanning electron micrograph of the fracture surface of the butterfly that would substantiate this fatigue mechanism.

Figure 30. Scanning Electron Micrograph of Fracture Surface of Broken Butterfly Connection. (The fatigue striae are clearly visible on the surface of the grains.)

IV. CONCLUSIONS

No failures were observed that could be attributed directly to the alumina substrate. Anticipated failures due to differential thermal expansion during heating/cooling and flexure of the substrate during vibration/shock were not seen.

The solder fillets at the components showed some mechanical work and minor cracking due to differential thermal expansion between the component and the substrate. However, this is to be expected with the number of thermal cycles the components experienced. The condition of the fillets after a total of 1000 cycles may be inferred from Figures 26 through 29. No open solder joints were experienced.

The absence of any solder joint failures in these tests is noteworthy in view of findings by Caruso, Allen, and Howard (Ref. 1) and Kinser, Vaughan, and Graff (Ref. 2). In each of these reports the conclusion is made that solder-bonded systems are too unreliable for military space systems. This conclusion is based on a high failure rate of the bonds in several environments, especially that of thermal cycling. Caruso, Allen, and Howard (Ref. 1) also commented on bond failures due to vibration and shock. Kinser et al. (Ref. 2) acknowledge the fact that, while their results generally indicated that solder failure was the major failure mechanism, some test substrates survived 1000 thermal cycles with no failures. They concluded that the major problem was reproducibility of the soldering technique.

---

[1] S. V. Caruso, R. V. Allen, and R. T. Howard, Investigation of Mounting Discrete Chip Components for Hybrid Microelectronic Applications, Report No. S&E-ASTR-RMH-73-1, NASA/MSFC (1973).

[2] D. L. Kinser, J. G. Vaughan, and S. M. Graff, "Reliability of Soldered Joints in Thermal Cycling Environments," Electronic Packaging and Production, pp. 61-68 (May 1976).

The results of the present work are, however, confirmed by similar studies conducted at TRW (Ref. 3), which are summarized briefly as follows:

a. Design Verification Test

Sixteen test alumina substrate assemblies containing 372 chip capacitors and 48 chip resistors all passed the test without a single failure. This test consisted of:

1. Thermal Cycling. The temperature limits were established by taking the worst case qualification requirements of all our programs and adding a 30°C margin pad to both the high and low temperature extremes. In determining the number of cycles, it was assumed that the most severe qualification testing requires 10 cycles and, in the worst case, three to four reworks would expose some equipment up to 30 and 40 cycles. By adding a safety factor of approximately 3, a figure of 100 cycles was established.

2. Vibration. Qualification level requirements are typically 0.2 g^2/Hz PSD from 100 to 1000 cycles with a 6-dB dropoff at both ends. Overstress testing by factors of 2, 3, and 4 are imposed to ensure a margin of safety.

3. Shock. By assuming a Q of 20 and a peak g at 5000 Hz, the test simulates pyrotechnic shock. Typical qualification levels are between 2500 and 5000 g's peak. The overstress at 10,000 g's is included to ensure a margin of safety.

b. Thermal Cycling to Failure

Eight substrates, after completing design verification testing, were subjected to a cumulative total of 400 thermal cycles from -50°C to +100°C and 100% passed visual and electrical test requirements. This indicates an excellent margin of safety. One substrate was metallographically cross-sectioned to determine the quality of the solder bond and metallization system bond after this stage of overstress. The solder joint and metallization system was shown to be intact and reliable.

After 1237 cycles, all parts passed electrical tests except one small capacitor, which opened at 820 cycles. This failure will be analyzed downstream.

---

[3] Alumina Substrate Assembly Technology at TRW Systems, TRW Systems, Redondo Beach, California (1974).

c. Operational Life Test

Ten substrates containing 240 chip capacitors (both ceramic and porcelain) have passed 7002 cycles from +40°F to +90°F. Testing was continued to 16,000 cycles.

TRW concluded from their test results that there is an excellent margin of safety in the ASA solder attach/metallization system to handle the stresses resulting from mismatch of thermal coefficient of expansion between TRW approved chip capacitors and TRW metallized alumina substrates.

Following a detailed failure analysis of capacitor C26, it was concluded that the cause of the failure was unknown. That is, it was felt that, based on extensive test data, the circumferential crack in the center of the ceramic body could not have been caused by the vibration, shock, or temperature cycling.

The crack that caused failure of capacitor C23 is located under the end cap. One cause for this type of failure has been suggested in preliminary work at TRW (Ref. 4). This study indicated that there is a definite correlation between this type of crack and the thickness of the copper barrier plating on the end cap for Union Carbide type BX capacitors. This failure can be observed to a greater or less degree in capacitors C23, C24, and C25 (Figures 26, 27, and 28 respectively). However, this failure mode was not observed with Union Carbide's NPO-type capacitors. This was confirmed in the present study in the cross section of unit C22 (Figure 29) which is of the NPO type. The intermittency in C24 could easily have resulted from cracking in the ceramic under the end cap or from the poor contacts in the end cap metallization.

By comparison, the cross sections of two capacitors that did not fail showed structures that were quite good. This would indicate that good capacitors will survive the conditions imposed on them during this test, but those units with any defects can be expected to fail.

---

[4] J. Woodward, TRW Systems, Redondo Beach, California, personal communication (1976).

The Piconics inductors should be expected to respond to the tests in the same manner as the capacitors. The wrap-around metallization that is soldered to the ASA is itself fabricated from alumina chips and, therefore, even a differential thermal expansion failure mechanism could not be present. The only failures observed with these inductors were due to defective welds during manufacture that could be "opened" as a result of differential thermal expansion between the alumina chip in the base and the diallyl phthalate molded body.

The only other failure observed was that of the one butterfly interconnect. This failure, however, can be traced to a loose tiedown bolt. Assuming that the proper torque is applied to each bolt, this type of failure should not occur.

In conclusion, it would appear that the alumina substrate assembly as described herein is a viable medium for the fabrication of electronic modules that are subjected to vibration, shock, and thermal cycling within the range of this study.

APPENDIX A

TEST REPORT NO. 5330-2134
RANDOM VIBRATION & PYROTECHNIC SHOCK
TEST REPORT
ON
ASA ELECTRONIC MODULES
P/N 283239-1, S/Ns 1, 2, & 3

APPROVED ENGINEERING TEST LABORATORIES

Report No. 5330-2134
P. O. No. 56315
Date: 3 April 1975

TESTED FOR

Aerospace Corporation
P. O. Box 95085
Los Angeles, California 90045

TEST ITEMS

ASA Electronic Modules, Part Number 283239-1, Serial Numbers 1, 2, & 3

TESTS PERFORMED

Random Vibration
Pyrotechnic Shock

REFERENCES

- Customer Instructions

TEST EQUIPMENT

AETL No.	Manufacturer	Instrument
Vibration Test		
D13L	M. B. Electronics	Control Console, M/N T388
D84L	M. B. Electronics	Vibration Exciter, M/N C150
D98L	Endevco Corp.	Accelerometer, M/N 2272
D113L	Moseley	X-Y Recorder, M/N 2D-2A
D148L	Unholtz Dickie	Charge Amplifier, M/N D11MGV-8
D149L	Unholtz Dickie	Charge Amplifier, M/N D11MGV-8
D151L	Ling	Amplifier, M/N PP75/90
D167L	Spectral Dynamics	Ensemble Averager, M/N SD302
D168L	Spectral Dynamics	Real Time Analyzer, M/N SD301A
D242L	Endevco Corp.	Accelerometer, S/N C472
E3043E	Ballantine Labs	True RMS Voltmeter, M/N 320U/6
ENV26L	Leeds & Northrup	Temperature Potentiometer, M/N 8693
Pyrotechnic Shock Test		
D38L	Plotamatic	X-Y Plotter, M/N 610
D84L	M. B. Electronics	Vibration Exciter, M/N C150
D148L	Unholtz Dickie	Charge Amplifier, M/N D11MGV-8
D151L	Ling	Amplifier, M/N PP75/90
D189L	M. B. Electronics	Shock Spectrum Analyzer, M/N N982-3
D197L	Endevco Corp.	Accelerometer, M/N 2225
E299L	Hewlett Packard	Plug In Unit, M/N 1405A
ENV26L	Leeds & Northrup	Temperature Potentiometer, M/N 8693

TEST PROCEDURES AND TEST RESULTS

Vibration Test

The bare test fixture, with no test specimens mounted on it, was mounted on the vibration exciter and was subjected to evaluation over the frequency range of 50 to 2000 Hz at an applied acceleration of 5.0 g peak. During the fixture evaluation, the outputs of the control and response acceletometers, mounted as illustrated in Figure 1, were recorded on X-Y plots. The X-Y plots are presented in Appendix 1. The bare test fixture was then subjected to fixture evaluation in each of the three major orthogonal axes over the frequency range of 20 to 2000 Hz using random vibration at the following intensities:

Frequency (Hz)	Intensity
20 - 100	6.0 db/octave rise
100 - 1000	1.0 g^2/Hz
1000 - 2000	6.0 db/octave rolloff
Overall Acceleration:	36.0 grms

The PSD plots obtained during fixture evaluation are presented in Appendix 2.

Each specimen, in turn, was then installed in a test fixture and was mounted on the vibration exciter. Each specimen was subjected to six minutes of random vibration in each of the three major orthogonal axes over the frequency range of 20 to 2000 Hz at the intensities noted above for the 36.0 grms level at temperatures of room ambient, -35°C, and +60°C.

Visual examination following testing in each axis revealed no damage or other adverse effects. The PSD plots are presented in Appendix 3.

Pyrotechnic Shock Test

Each specimen, in turn, was installed in a test fixture and was mounted on the vibration exciter. Each specimen was subjected to one synthesized shock pulse in each direction of the three major orthogonal axes. Each shock pulse had an amplitude of 2500 g, at a a peak frequency of 10,000 Hz.

Testing was performed at temperatures of room ambient, -35°C, and +60°C. Visual examination following testing in each direction revealed no damage or other adverse effects. X-Y plots of the shock pulses are presented in Appendix 4.

TEST PROCEDURES AND TEST RESULTS (Cont.)

Pyrotechnic Shock Test (Cont.)

NOTE: The test equipment used; i.e., a vibration exciter, resulted in the plus and minus directions of testing being performed simultaneously during each applied pulse.

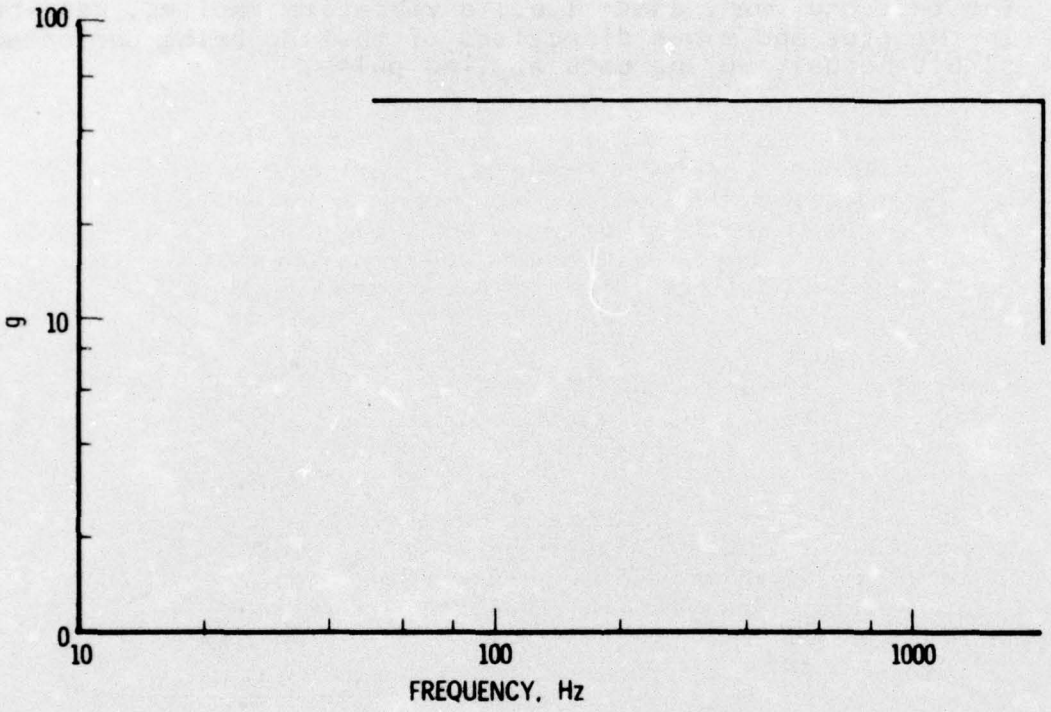

Figure A-1. Typical Calibration Curve for Control Accelerometer Used in Vibration Test, Phase I

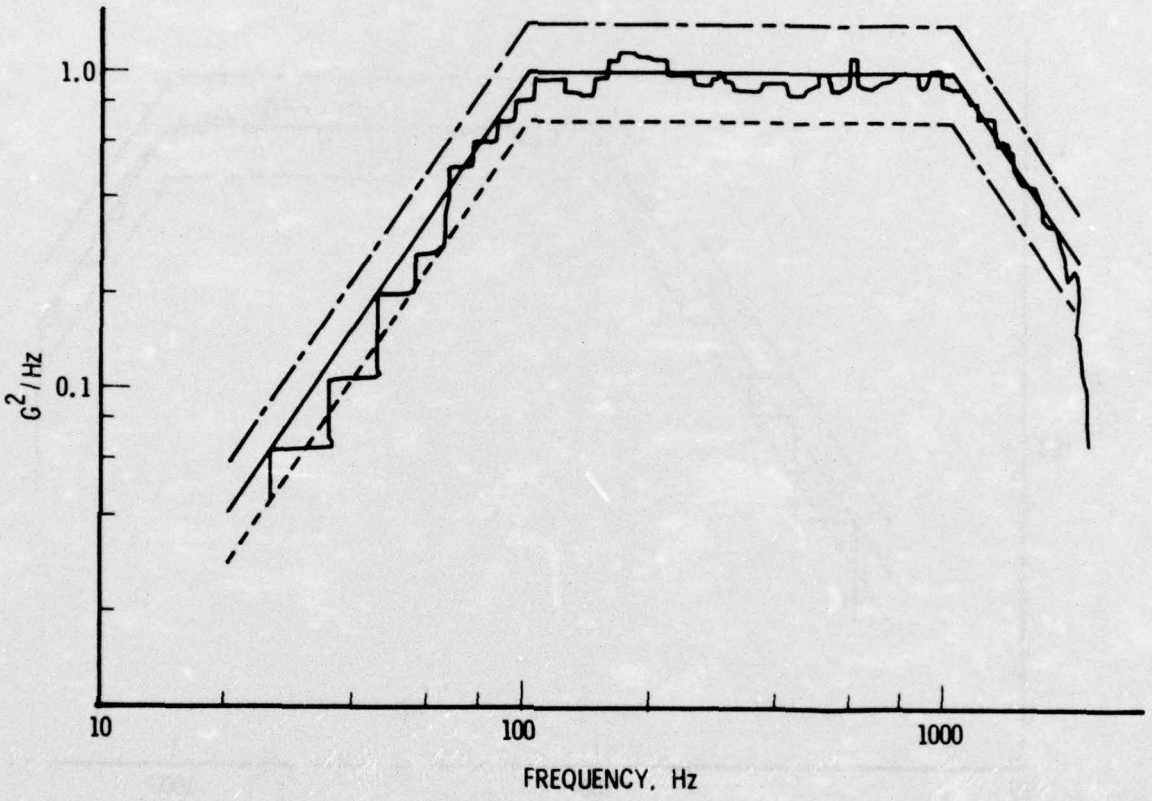

Figure A-2. Typical PSD Curve for Fixture Evaluation in Vibration Test, Phase I

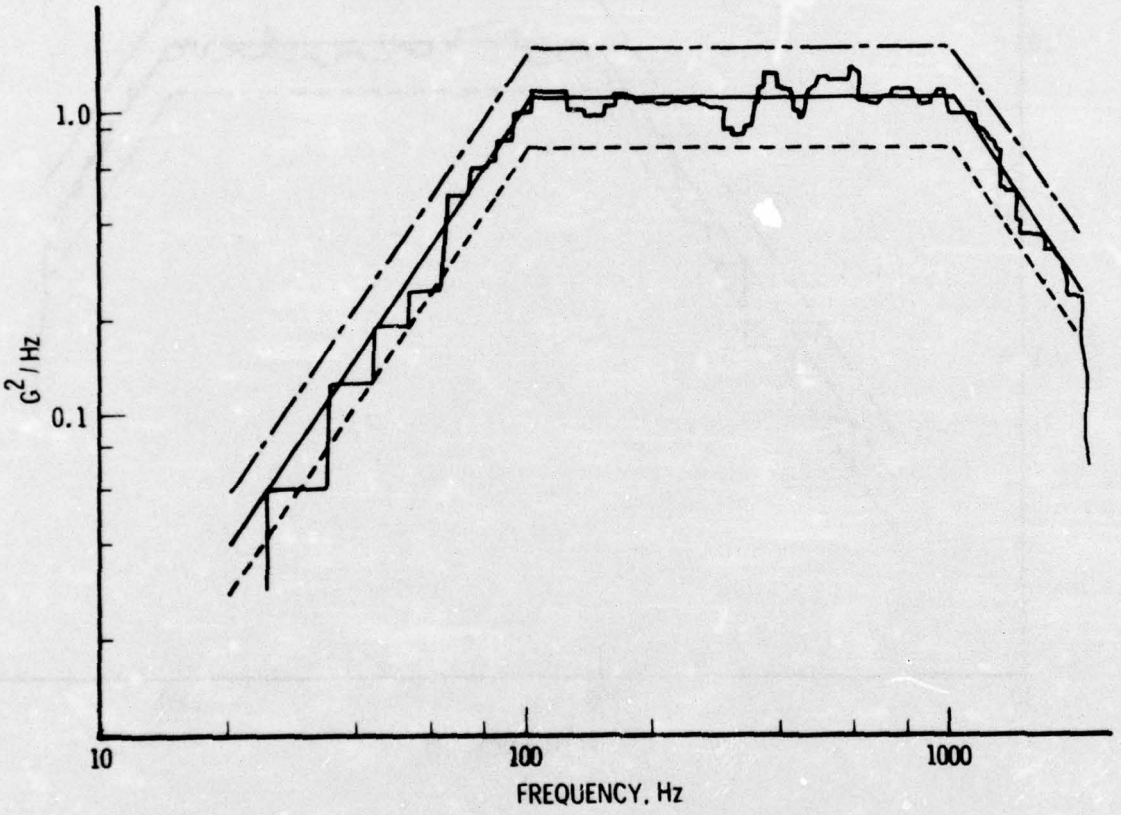

Figure A-3. Typical PSD Curve for ASA Module, Phase I

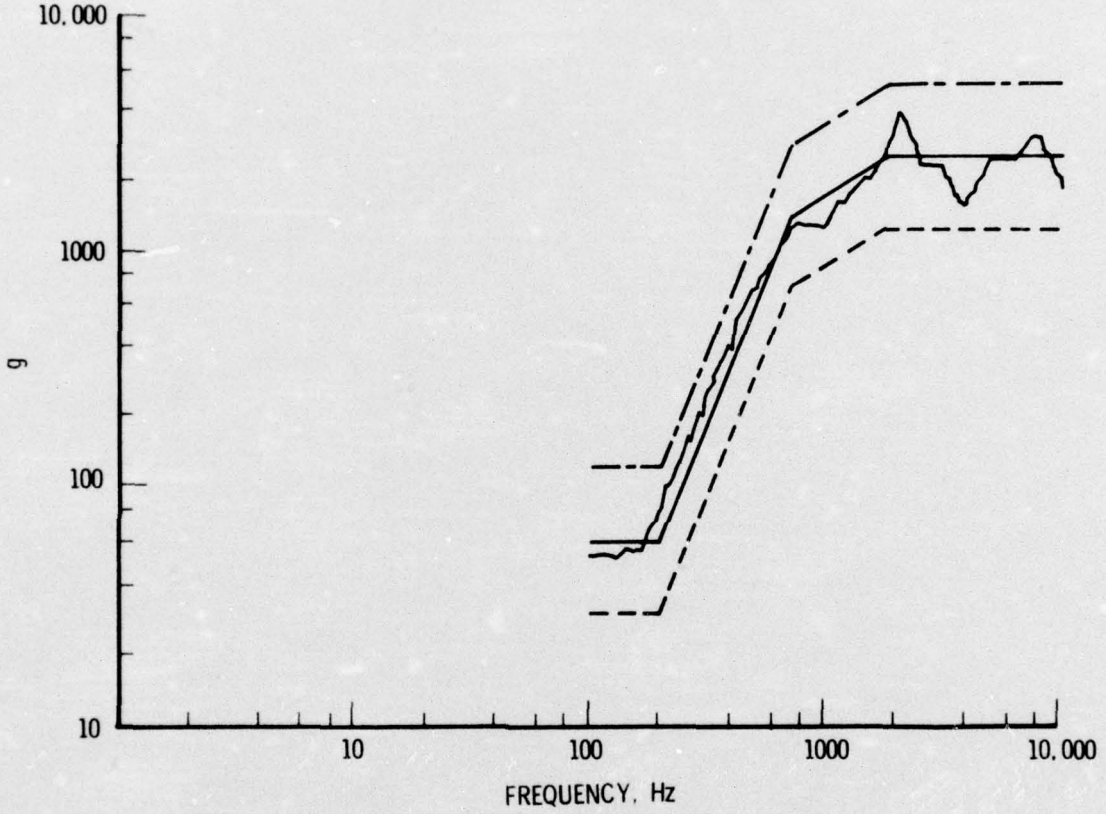

Figure A-4. Typical Curve for the Pyrotechnic Shock Applied to the ASA Module, Phase I

APPENDIX B

TEST REPORT NO. 5330-2716
ASA ELECTRONIC MODULE
P/N 283259-1, S/N 002

APPROVED ENGINEERING TEST LABORATORIES
Los Angeles Division

Report No. 5330-2716
P. O. No. 65911
Date: 23 January 1976

9 Page Report

Aerospace Corporation
P. O. Box 92957
Los Angeles, California 90009

TEST ITEM

ASA Electronic Module, Part Number 283259-1, Serial Number 002

SUMMARY

This report certifies that the test specimen identified above has been subjected to Random Vibration and Pyrotechnic Shock Testing in accordance with customer instructions. No adverse effects were noted.

TEST EQUIPMENT

AETL No.	Manufacturer	Instrument
Vibration Test		
D84L	M. B. Electronics	Vibration Exciter, M/N C150
D113L	Moseley	X-Y Recorder, M/N 2D-2A
D140L	Ballantine Labs	True RMS Voltmeter, M/N 320
D148L	Unholtz Dickie	Charge Amplifier, M/N D11MGV-8
D151L	Ling	Amplifier, M/N PP75/90
D167L	Spectral Dynamics	Ensemble Averager, M/N SD302
D168L	Spectral Dynamics	Real Time Analyzer, M/N SD301A
D218L	Bruel & Kjaer	Accelerometer, M/N 4335
D348L	M. B. Electronics	Control Console, M/N T589
Pyrotechnic Shock Test		
D19L	Ballantine Labs	True RMS Voltmeter, M/N 320
D20L	Moseley	X-Y Plotter, M/N 135R
D84L	M. B. Electronics	Vibration Exciter, M/N C150
D148L	Unholtz Dickie	Charge Amplifier, M/N D11MGV-8
D151L	Ling	Amplifier, M/N PP75/90
D189L	M. B. Electronics	Shock Spectrum Analyzer, M/N N982-3
D197L	Endevco Corp.	Accelerometer, M/N 2225
D331L	M. B. Electronics	Shock Spectrum Synthesizer, M/N N981

TEST PROCEDURES AND TEST RESULTS

Random Vibration Test

The specimen was installed in a test fixture and was mounted on the vibration exciter. The specimen was subjected to six minutes of random vibration in the vertical axis over the frequency range of 20 to 2000 Hz at the following intensities:

TEST PROCEDURES AND TEST RESULTS (Cont.)

Random Vibration Test (Cont.)

Frequency (Hz)	Intensity
20 - 100	6 db/octave rise
100 - 1000	1.0 g^2/Hz
1000 - 2000	6 db/octave rolloff
Overall Acceleration:	36.0 grms

Visual examination following testing revealed no damage or other adverse effects. The PSD plots are presented in Appendix 1.

Pyrotechnic Shock Test

The specimen was installed in a test fixture and was mounted on the vibration exciter. The specimen was subjected to one pyrotechnic shock in each direction of the lateral axis. The shock pulse had an amplitude of 2500 g at a peak frequency of 10,000 Hz.

Visual examination following testing in the lateral axis revealed no damage or other adverse effects. The X-Y plots of the shock pulses are presented in Appendix 2.

NOTE: The test equipment used; i.e., a vibration exciter, resulted in the plus and minus directions of testing being performed simultaneously during each applied pulse.

AETL QC

STATE OF CALIFORNIA
COUNTY OF LOS ANGELES } ss

DEANE HELLER, Project Manager being duly sworn, deposes and says: That the information contained in this report is the result of complete and carefully conducted tests and is to the best of his knowledge true and correct in all respects.

Deane Heller

SUBSCRIBED and sworn to before me this 23 day of January, 19 76

Karl G. Schmidt
Notary Public in and for the County of Los Angeles, State of California.

OFFICIAL SEAL
KARL G. SCHMIDT
NOTARY PUBLIC-CALIFORNIA
LOS ANGELES COUNTY
My Commission Expires Sept. 22, 1977

2

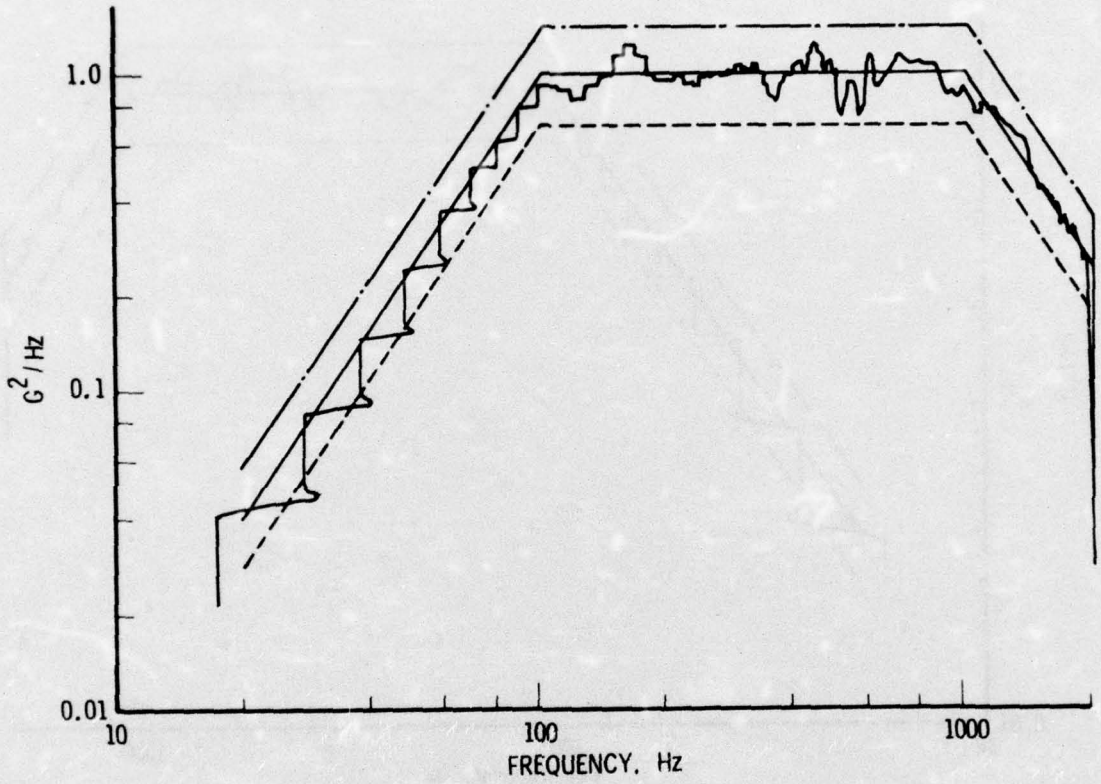

Figure B-1. Typical PSD Calibration Curve for Fixture Evaluation in Vibration Test, Phase II

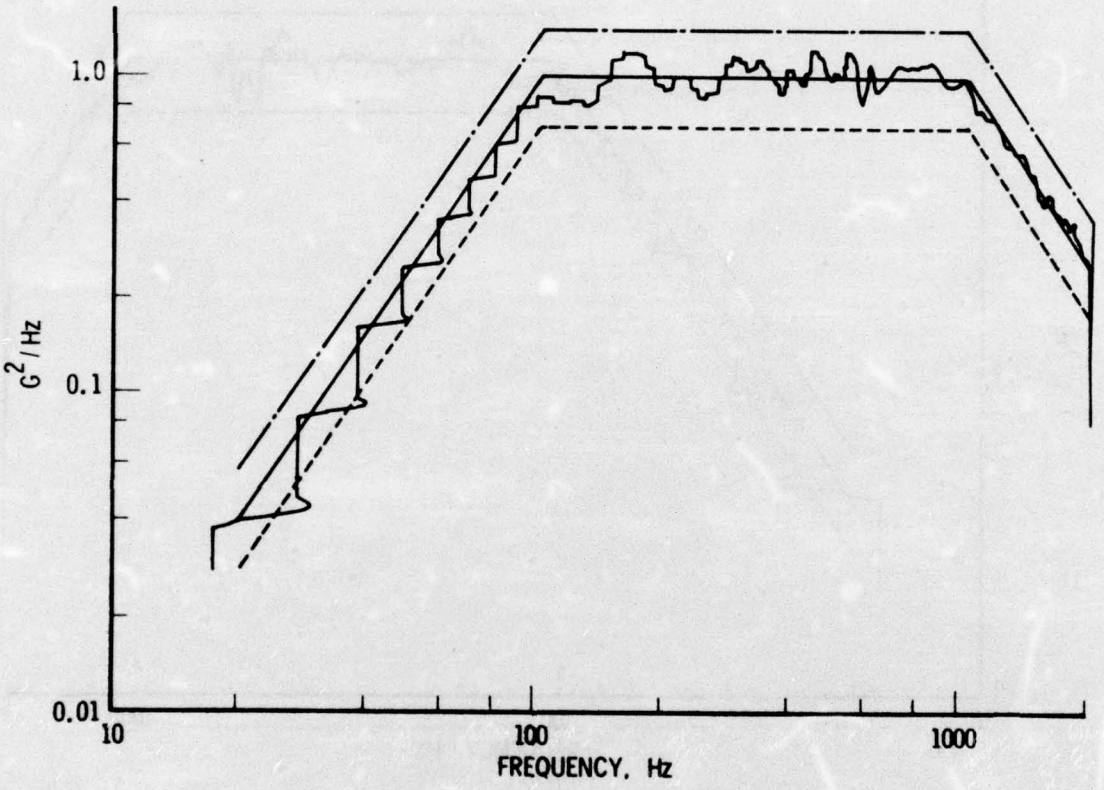

Figure B-2. Typical PSD Curve for ASA Module, Phase II

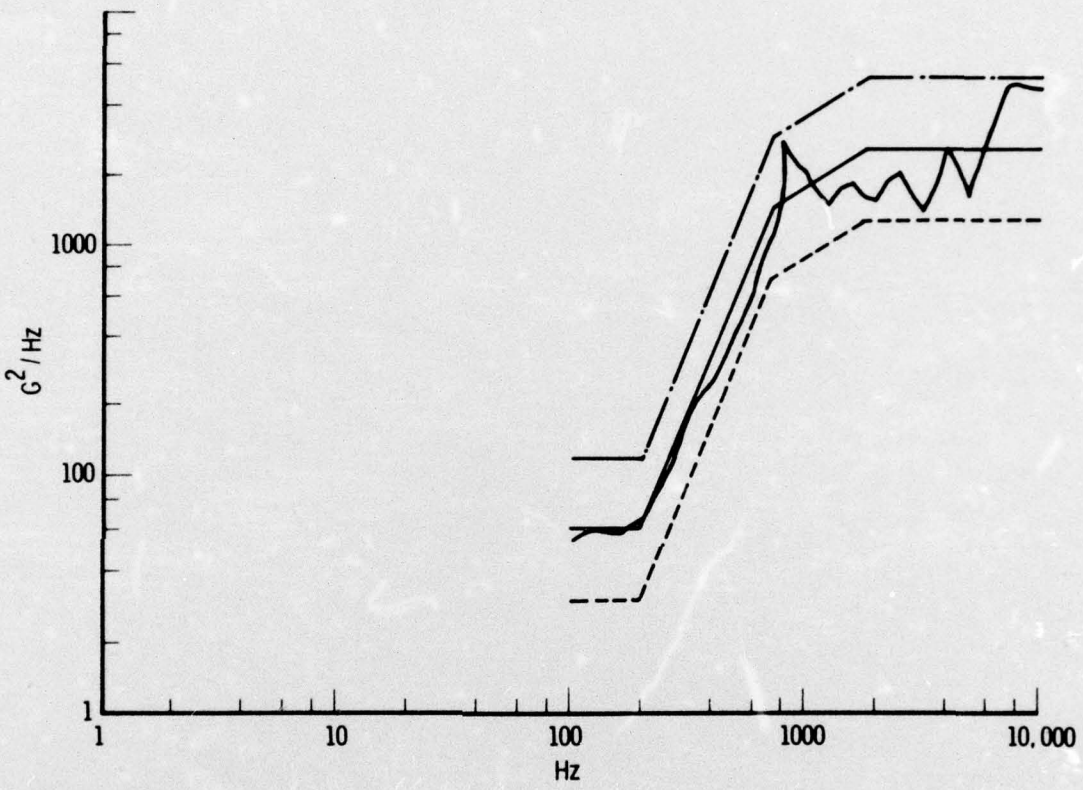

Figure B-3. Typical Curve for the Pyrotechnic Shock Applied to the ASA Module, Phase II

APPENDIX C

IOC NO. 7511-2745/75
UNION CARBIDE CHIP CAPACITOR FAILURE
ON AEROSPACE TEST MODULE

TRW
SYSTEMS GROUP

R.D. Engquist

INTEROFFICE CORRESPONDENCE 7511-2745/75

TO H. Sabath CC Distribution DATE May 21, 1975

JUN 5 RECD
D. L FRESH

SUBJECT Union Carbide Chip Capacitor Failure on Aerospace Test Module

FROM J. Woodward
BLDG R6 MAIL STA. 2134 EXT. 50556

Reference: 7511-684/73, "Thermal Shock of Alumina Substrate Assemblies", J.P. Woodward to Distribution, 7 February 1973.

A "D" case size Union Carbide capacitor was found to be electrically open shortly after commencing temperature cycling from -50°C to +100°C in the subject environmental test program. The test modules had previously been subjected to vibration, shock and 200 temperature cycles from -35°C to +60°C. The capacitor chain which contained the subject capacitor had exhibited intermittent noise during the vibration and shock testing but had performed normally through-out the subsequent temperature cycling from -35°C to +60°C.

After the electrical open was observed, the capacitor chain was examined by Aerospace Corp. and a crack in the subject capacitor was found (Figures 1-3). The module was delivered to TRW and the capacitor was removed intact. The crack was evident on all 4 sides of the capacitor (Figures 4-7). Metallographic cross-sectioning revealed that the crack extended completely through the part (Figures 8-10). It is possible that unfractured internal metallization layers held the part intact.

The components were electrically monitored continuously through-out the test. The subject capacitor chain exhibited minor noise (15 mV) during Z axis vibration at room temperature. The noise increased to 50 mV during Z axis vibration at temperature extremes(-35°C and +60°C). The noise continued in the X axis but was not observed in the Y axis. During shock testing (2500 Gs), the electrical noise increased until it exceeded a 300 mV change (went off scale); erratic readings were recorded during the 30 minute recovery period.

The cause of the failure is unknown. The crack in the chip is identical to those observed in "D" case Union Carbide capacitors subjected to thermal shock (Ref). However, no chip capacitors have failed in TRW vibration or shock testing (up to 10,000 Gs), except in those cases

where uncontrolled test conditions caused excessively high G forces. Consequently, failure could be the result of some type of thermal shock, a combination of vibration and temperature extremes (a condition not tested by TRW) or the part could have been defective. A visual examination of the part revealed no evidence of external defects. It is inconceivable that vibration, shock, or temperature cycling caused the failure based on the extensive test data gathered by TRW.

No further investigation will be performed at this time.

J. Woodward
Metallic Materials Section
Materials & Processes Dept.

JW/jsh

Distribution

A. Dozier	R6/2134
C. Holzbauer	R6/2114
R. Luirette	M5/1470
P. Pavesi	R6/2188
R. Perrin	R6/2591
J. Reames	R6/0869
B. Spanier	R6/2108
E. Thornley	R6/2591

NOTE: The figures referenced in this appendix are not included here because reproducible copy of the material is not available.

APPENDIX D

IOC NO. 7511-2642/75A
FAILURE ANALYSIS
1R002-012V PICONICS VARIABLE INDUCTORS
INSTALLED IN AEROSPACE TEST MODULES

TRW SYSTEMS GROUP

R.D. Engquist

INTEROFFICE CORRESPONDENCE

7511-2642/75 A

TO: H. Sabath CC: Distribution DATE: April 22, 1975

SUBJECT: Failure Analysis, 1R002-012V Piconics Variable Inductors Installed in Aerospace Test Modules

FROM: K. Kono/J. Woodward
BLDG R6 MAIL STA. 2134 EXT. 50[illegible]

References: 1) ASA Test Modules for Aerospace Corp. SN 26143.000

2) 7570.4-108, "Status of ASA Test Module for Aerospace Corp.", H. Sabath to A.B. Graybill/R.B. Luirette, 21 March 1975.

3) 7511-2579/75, "Electrical Open in Aerospace ASA Test Module", J. Woodward to H. Sabath, 1 April 1975.

4) 5215.5-75-73 (Aerospace Corp.), "ASA Test Program", J.J. Egan to Distribution, 1 April 1975 (ATTACHED).

5) 7570-110, "Request for MSO to Rework Aerospace Corp. ASA Test Module", H. Sabath to F. Knight, 3 April 1975.

6) FAR5-050, Analysis of 1R002-012V-001 Piconics Variable Inductors, 4 April 1975.

INTRODUCTION

Aerospace Corp. requested that representative modules be assembled for a verification test program to be conducted by Aerospace Corp. in support of the FSC program. Reference 1 documents the test program. Three modules consisting of six alumina substrate assemblies were built using standard TRW parts and procedures. The test modules were then delivered to Aerospace Corp. for environmental testing consisting of random vibration, simulated pyrotechnic shock and temperature cycling.

The test modules survived the vibration and shock exposures.

After 71 temperature cycles electrical anomalies were recorded in the inductor chain of module S/N 003. The anomaly initially exhibited

evidence of an intermittant open. As temperature cycling progressed the intermittant condition progressively worsened. The symptoms of the condition were:

a. Open circuit condition at low temperatures.

b. Noise (instability) during transistion to high temperature.

c. Normal behavior at high temperatures.

After 200 temperature cycles, TRW (H. Sabath and J. Woodward) received an invitation from Aerospace Corp. to witness the X-ray, electrical testing and the opening of the test modules (Reference 2).

A visual examination of module S/N 003 and a review of the inductor X-rays revealed no indications of the cause of the electrical anomaly. Electrical D.C. measurements of the inductor chain confirmed the existance of an open and further testing isolated one inductor that was "open" and another that was "intermittant". Both inductors were variable inductors per the TRW PIN 1R002-012V-001.

A meeting was held at TRW (Reference 3) at which the potential failure modes were discussed and a recommendation was adopted that the two failed inductors be removed from the substrates, electrically tested, X-rayed and subjected to destructive metallographic examination. The failure analysis was to be performed by TRW and the test module returned to Aerospace Corp. for additional temperature cycling. Aerospace Corp. agreed with the recommendations (Reference 4).

The subject parts were removed from the substrates using standard ASA soldering procedures and the vacant pads were hard-wired. The rework was accomplished using a special rework MSO (Reference 5).

After the parts were removed, electrical tests confirmed that the anomalies were symptoms of defects in the inductors and not the alumina substrates.

The removal and electrical testing was witnessed by A. Young of Aerospace Corp.

GENERAL

The TRW PIN 1R002-012V-001 device is a variable RF coil with inductances adjustable between 0.750 to 1.20 μ H and is one of a series of twelve variable inductors of comparable construction manufactured by Piconics Inc.

The dimensions and general external construction features are shown in Figure 1.

Figure 2 is an X-ray view of the 1R002-012 device and shows the internal coil configuration of the device.

The general fabrication processes for the device are as follows:

1. Magnet wire (Bridgeport Insulated Wire Co., Polynylon Bond, MIL-W-583, Class 130) is wound on a mandrel and the coil ends are trimmed, stripped and dressed. A chemical stripper (Fidelity Chemical, Super X-Var) is used to strip and alcohol is used to clean the stripped coil ends.

2. The mandrel is positioned on the substrate and its end bonded to the center of the substrate with Castall 251 (RT-1, hardener) epoxy system.

3. The stripped ends of the coil are parallel gap welded to the substrate bonding pads. A Hughes Model MCW-550 power supply and Model VTA-66 welding head are used in the welding operation.

4. The coil is conformally coated with the Castall 251 (RT-1, hardener) epoxy system.

5. The inductor body is injection molded with glass fiber filled diallyl phthalate.

6. The coil mandrel is removed.

The wire sizes used in the various devices of the series are as listed in Table I. Also listed in Table I are the diameters and the cross-sectional areas of the wires.

The 1R002-012 device uses a 2 mil diameter wire for its coil. All other devices use wires of larger diameters. Although the next larger wire diameter is only 0.5 mil larger at 2.5 mils, the cross-sectional area of the wire is roughly 55% greater and represents a substantial increase in mechanical strength.

The failure mode exhibited by the subject devices indicated an open condition in the device circuit. The following elements constitute the circuit path:

a. The "moly-manganese" thick film type metallization of the alumina chip substrate.

b. The nickel-gold plating over the "moly-manganese" base metallization.

c. The parallel gap weld between the magnet wire coil ends and the metallization of the alumina chip.

d. The magnet wire coil.

FAILURE ANALYSIS PROCEDURE

The two devices presented for analysis were identified as:

1. "Open" - From output substrate on circuit pads nearest the connector J8.

2. "Intermittent" - From input substrate on circuit pads most distant from connector J4.

The initial step in the analysis was to X-ray the devices. X-rays were taken from the three orthogonal directions in the Faxitron 804 X-ray unit. The limited resolution of the X-ray technique did not allow isolation of the failure mode. At best the X-ray allowed only the determination of the coil location and configuration and the location of the welds joining the ends of the coil to the alumina substrate (Figure 2).

The second step of the analysis was to establish continuity of the metallization system of the alumina substrate between the exposed solder coated areas of the chip and the weld bonding pad areas hidden by the diallyl phthalate molded body. This was accomplished by an examination of metallographic cross-sections of the chip metallization in the wrap-around areas.

Figure 2 shows the locations of the wrap-around metallization on the "open" device. Figure 3 is a photomicrograph of a typical metallographic cross-section of the wrap-arounds in the "open" device. It shows metallization continuity between the exposed and hidden areas of the metallization of the alumina chip.

Figure 4 is an X-ray of the "intermittant" device and shows the location of the wrap-around areas of this device. Figure 5 is a photomicrograph of a typical metallographic cross-section of the wrap-arounds in the "intermittant" device. It shows metallization continuity between the exposed and hidden areas of the metallization of the alumina chip.

The next step in the analysis was a metallographic examination of the welds and their immediate vicinity. To accomplish this, it was necessary to accurately determine the weld location and orientation. X-rays of the plan view of the welds were made after the metallization at the bottom exposed surfaces of the chips and the upper 1/3 of the molded body were removed.

After the locations and orientation of the welds were confirmed, successive metallographic cross-sections were prepared for each weld until the weld was completely traversed or until evidence of the failure mode was revealed.

Figure 6 is an X-ray view of the weld locations of the "open" devices. The welds are identified identically as in Figure 2.

Figure 7 is a typical cross-section of weld A in the "open" device. No defects were noted in the successive cross-sections of this weld.

Figure 8 is a cross-section of weld B of the "open" device. It shows a definite discontinuity in the wire between the weld and the coil. Figure 9 is a highly magnified photomicrograph of the crack. It shows evidence that the crack is filled with epoxy.

Figure 10 is an X-ray view of the weld locations of the "intermittant" device. The welds are identified identically as in Figure 4.

Figure 11 is a typical cross-section of weld C in the "intermittant" device. No defects were noted in the successive cross-sections of this weld.

Figure 12 is a cross-section of weld D of the "intermittant" device. It shows a definite discontinuity in the wire between the weld and the coil.

Figure 9 is a highly magnified photomicrograph of the crack. Although the presense of epoxy is not clearly evident in the photomicrograph,examination of the sample under the metallograph clearly shows that this crack is also filled with epoxy.

The cross-sections of the metallization on the alumina chips showed no evidence of discrepancies in the conductive layers.

The evidence indicated good adhesion between the "moly-manganese and the alumina and between the gold-nickel and the "moly-manganese". Distinct gold and nickel layers are not distinguishable in these devices because the substrate vendor (Centralab) exposes the substrates to elevated temperatures to enhance plating adhesion causing the two platings to diffuse into each other.

The weld interfaces of the wire to the metallization showed evidence of acceptable coherence in the weld.

DISCUSSION

The evidence found in the analysis indicates that the failures resulted from discontinuities in the magnet wire between a weld and the coil.

The discontinuities in each case occurred in the immediate vicinity of the inner (nearest the coil) edge of the inner parallel gap weld foot print.

The crack in each case showed evidence of being filled with epoxy.

The cross-section of the wire in each case indicated that the wire was sharply bent.

Figure 14 is a sketch showing the suspected initial condition of the failed interconnects.

In figure 14 are also shown the approximate locations of the cross-sections shown in Figures 8 and 12.

The suspected initial condition is believed to have resulted during the device assembly during or after the welding operation.

Such a condition might result from insufficient slack in the wire during welding or an excessive handling force on the wire after welding.

The suspected initial condition is the most plausible explanation consistant with presense of epoxy in the crack crevice. The epoxy is believed to have entered the crack during the conformal coating operation (See step 4, general fabrication processes).

It is not difficult to imagine how such a condition could progress to a complete separation of the magnet wire due to the strain imposed on the initial crack by the repeated stresses resulting from the differences in thermal coefficient of expansion of the materials used in the construction of the device.

K. Kono
Metallic Materials Section
Materials & Processes Dept.

J.P. Woodward
Metallic Materials Section
Materials & Processes Dept.

KK/JPW/js

TABLE I

1R002 Inductors: Coil Wire Sizes

PIN Number	Gage (AWG)	Diameter ($X10^{-3}$ inches)	Cross-Sectional Area ($X10^{-6}$ inches^2)
1R002-001	32	8.0	47.00
-002	34	6.3	31.20
-003	33	7.1	39.60
-004	34	6.3	31.20
-005	32	8.0	47.00
-006	37	4.5	15.90
-007	38	4.0	12.60
-008	39	3.5	9.60
-009	38	4.0	12.60
-010	42	2.5	4.90
-011	42	2.5	4.90
-012	44	2.0	3.15

NOTE: The figures referenced in this appendix are not included here because reproducible copy of the material is not available.

GLOSSARY

AETL	Approved Engineering Test Laboratories
ASA	Alumina Substrate Assembly
CLA	centerline average
CPH	cycles per hour
DPA	destructive physical analysis
DVM	digital voltmeter
L/R	inductance-resistance
PSD	power spectral density
R/C	resistance-capacitance
rms	root mean square
SEM	scanning electron microscope